THE JOURNAL OF BIOLOGICAL CHEMISTRY VOL. 291, NO. 33, pp. 17209–17227, August 12, 2016

Amyloid Precursor Protein (APP) May Act as a Substrate and a Recognition Unit for CRL4^{CRBN} and Stub1 E3 Ligases Facilitating Ubiquitination of Proteins Involved in Presynaptic Functions and Neurodegeneration*

Received for publication, April 21, 2016, and in revised form, June 7, 2016 Published, JBC Papers in Press, June 20, 2016, DOI 10.1074/jbc.M116.733626

Dolores Del Prete[‡], Richard C. Rice[§], Anjali M. Rajadhyaksha[§¶], and Luciano D'Adamio[‡1]

From the [‡]Department of Microbiology and Immunology, Albert Einstein College of Medicine, Bronx, New York 10461 and the [§]Division of Pediatric Neurology, Department of Pediatrics, and [¶]Feil Family Brain and Mind Research Institute, Weill Cornell Autism Research Program, Weill Cornell Medical College, New York, New York 10065

The amyloid precursor protein (APP), whose mutations cause Alzheimer disease, plays an important *in vivo* role and facilitates transmitter release. Because the APP cytosolic region (ACR) is essential for these functions, we have characterized its brain interactome. We found that the ACR interacts with proteins that regulate the ubiquitin-proteasome system, predominantly with the E3 ubiquitin-protein ligases Stub1, which binds the NH_2 terminus of the ACR, and CRL4^{CRBN}, which is formed by Cul4a/b, Ddb1, and Crbn, and interacts with the COOH terminus of the ACR via Crbn. APP shares essential functions with APP-like protein-2 (APLP2) but not APP-like protein-1 (APLP1). Noteworthy, APLP2, but not APLP1, interacts with Stub1 and CRL4^{CRBN}, pointing to a functional pathway shared only by APP and APLP2. *In vitro* ubiquitination/ubiquitome analysis indicates that these E3 ligases are enzymatically active and ubiquitinate the ACR residues Lys$^{649/650/651/676/688}$. Deletion of Crbn reduces ubiquitination of Lys^{676} suggesting that Lys^{676} is physiologically ubiquitinated by CRL4^{CRBN}. The ACR facilitated *in vitro* ubiquitination of presynaptic proteins that regulate exocytosis, suggesting a mechanism by which APP tunes transmitter release. Other dementia-related proteins, namely Tau and apoE, interact with and are ubiquitinated via the ACR *in vitro*. This, and the evidence that CRBN and CUL4B are linked to intellectual disability, prompts us to hypothesize a pathogenic mechanism, in which APP acts as a modulator of E3 ubiquitin-protein ligase(s), shared by distinct neuronal disorders. The well described accumulation of ubiquitinated protein inclusions in neurodegenerative diseases and the link between the ubiquitin-proteasome system and neurodegeneration make this concept plausible.

Processing of APP[2] plays an important role in the central nervous system. A polymorphism in *APP* that reduces APP processing protects from sporadic Alzheimer disease (AD) (1). In contrast, mutations in *APP* and in genes that regulate APP processing, such as *PSENs* and *BRI2/ITM2B*, cause familial dementias (2–12). APP is cleaved by β-secretase/BACE1 into a soluble ectodomain (soluble APPβ) and the COOH-terminal fragment β-CTF. Alternatively, α-secretase cleaves APP into soluble APPα and a shorter COOH-terminal fragment, α-CTF. β-CTF and α-CTF can be cleaved by γ-secretase to produce Aβ and the APP intracellular domain (AID) or P3 and AID, respectively (13–17). AID contains the ACR plus a few amino acids derived from the trans-membrane region of APP. AID is released in the cytosol upon production. Another processing pathway involves cleavage of APP in the ACR by caspase-6, -3, and -8 (18–24). Sequential γ-secretase/caspase processing can potentially generate the NH_2- and COOH-terminal cytosolic peptides JCasp and Ccas (23, 24).

In vivo studies have identified an essential role for the ACR in the patterning of neuromuscular junction and survival and in synaptic transmission (25–29). Other studies have suggested that release of AID modulates apoptosis, gene transcription, and Ca^{2+} homeostasis (23, 30–40). The caspase-derived APP fragments Ccas and JCasp also possess toxic activities (22–24). Overall, these data indicate that the ACR is functionally important *in vivo*.

APP belongs to a protein family that includes APLP1 and APLP2. APLP1 and APLP2 are processed like APP (41–45) and release intracellular peptides, called ALID1 and ALID2, respectively, that, like AID, can potentially regulate transcription (42, 46). The evidence that *Aplp2*-KO and *App*-KO mice are viable and show normal synaptic vesicle release, whereas the combined *App/Aplp2*-dKO mice develop neuromuscular junction deficits, die shortly after birth, and have altered synaptic vesicle exocytosis (28, 47), illustrates the functional redundancy of APP and APLP2.

The ACR is short and does not possess enzymatic activity, suggesting that it may function by modulating the activity of interacting proteins. As discussed above, several APP metabo-

* This work was supported by National Institutes of Health Grants R01AG033007, R01AG041531, R21AG048971, and R01AG052286 from NIA (to L. D.), The Hartwell Foundation (to A. M. R.), and The BrightFocus (to D. D. P.). The authors declare that they have no conflicts of interest with the contents of this article. The content is solely the responsibility of the authors and does not necessarily represent the official views of the National Institutes of Health.

[1] To whom correspondence should be addressed. E-mail: luciano.dadamio@einstein.yu.edu.

[2] The abbreviations used are: APP, amyloid precursor protein; AD, Alzheimer disease; ACR, APP cytosolic region; UPS, ubiquitin-proteasome system; BisTris, 2-[bis(2-hydroxyethyl)amino]-2-(hydroxymethyl)propane-1,3-diol; WB, Western blotting; CRL, Cullin-RING ubiquitin ligase; K-Ub, lysine residues ubiquitinated; dKO, double knock-out; DUB, deubiquitinating enzyme; NSAF, normalized spectral abundance factor; CTF, COOH-terminal fragment; AID, APP intracellular domain.

lites contain the ACR. These include the membrane-bound full-length APP, β-CTF, and α-CTF and the soluble AID peptide. Thus, complexes formed by ACR-interacting proteins may have distinct functional properties depending on the ACR-containing APP metabolite with which they interact.

Using an unbiased proteomic approach, we have characterized the ACR brain interactome (28, 48). Here, we show that the ACR interacts with several proteins that regulate the UPS. The E3 ubiquitin-protein ligase Stub1 and the E3 ubiquitin-protein ligase complex $CRL4^{CRBN}$, which is formed by Cul4a/b, Ddb1, and Crbn (49), are the most abundant UPS-related proteins interacting with the ACR. By performing ubiquitome analysis on the ACR brain interactome and total mouse brain, we generated evidence implicating APP in the ubiquitination of ACR-interacting proteins, and E3 ubiquitin-protein ligases, including $CRL4^{CRBN}$, in the ubiquitination of APP. Moreover, we found that APLP2, but not APLP1, can potentially exert a similar role. Finally, we observed that several of the UPS-related ACR interactors and proteins ubiquitinated *in vitro* in an ACR-dependent manner are genetically linked to neurodegeneration.

Ubiquitination can either modulate protein function or promote protein degradation by the proteasomal and the autophagic/lysosomal pathway. Integrity of these two pathways is important for normal aging and to ensure efficient turnover of both functional and defective proteins. The finding that APP may play a role in the ubiquitination of proteins linked to neurodegenerative diseases suggests that dysregulation of a functional network in which APP functions as a modulator of E3 ubiquitin-protein ligase(s) could be a pathogenic mechanism shared by numerous neuronal disorders.

Results

APP Interacts, via Its ACR, with Proteins That Regulate the UPS—In vivo observations underscore a key physiological and pathological role of the ACR (25, 27–29, 48, 50, 51, 53, 54). This short sequence lacks enzymatic activity and may function as a docking domain for cytosolic as well as membrane-bound proteins (46, 55–72). To explore the potential role of the ACR, we used a proteomic approach (28, 48). Five synthetic peptides, *i.e.* control St peptide, St-ACR, St-ACR with on Tyr^{682} (St-$ACR^{Tyr(P)}$), St-ACR with phosphorylation on Thr^{668} (St-$ACR^{Thr(P)}$), and St-ACR with phosphorylation on both Thr^{668} and Tyr^{682} (St-$ACR^{Thr(P)Tyr(P)}$), were immobilized on StrepTactin resin. The numbering of phosphorylated residues is based on the APP isoform of 695 amino acids. Mouse brain fractions were first passed twice through StrepTactin resin columns to remove proteins that bind to the StrepTactin resin. Then, they were applied in parallel on separate columns packed with either StrepTactin-St-, StrepTactin-St-ACR-, StrepTactin-St-$ACR^{Thr(P)}$-, StrepTactin-St-$ACR^{Tyr(P)}$-, or StrepTactin-St-$ACR^{Thr(P)Tyr(P)}$-coated resin. After extensive washing, the St, St-ACR, St-$ACR^{Thr(P)}$, St-$ACR^{Tyr(P)}$, and St-$ACR^{Thr(P)Tyr(P)}$ peptides were eluted, together with proteins specifically bound to them, with desthiobiotin. Eluted proteins were digested with trypsin and identified by nano-LC/MS/MS. We used St-ACR, St-$ACR^{Thr(P)}$, St-$ACR^{Tyr(P)}$, and St-$ACR^{Thr(P)Tyr(P)}$ peptides for two reasons. First is to identify interactions that are regulated by phosphorylation on these two residues. This goal is justified by previous reports showing that phosphorylation of either Thr^{668} or Tyr^{682} can modulate interaction of APP with some binding partners (73). Second is that the use of four independent ACR baits can help to pinpoint interactions that are possibly biologically relevant.

Analysis of proteins that interact with at least one St-ACR bait but not with the St control showed that the ACR can potentially interact with several proteins involved in the UPS. These include the following: 1) ubiquitin-like modifier-activating enzyme E1 and ubiquitin-conjugating enzyme E2 (Table 1); 2) E3 ubiquitin-protein ligase or components of E3 protein ligase complexes (Table 1); 3) proteins that regulate the E3 ligase activity (Table 2); 4) proteasome subunits (Table 2); 5) deubiquitinase; and 6) ubiquilins. Ubiquitin-like modifier-activating enzyme E1 (Uba1) and ubiquitin-conjugating enzyme E2-O (Ube2o) and E2-R2 (Ube2r2) were found in St-ACR pulldowns.

Nineteen E3 ubiquitin-protein ligases were found in St-ACR pulldowns as follows: Arih1, Hecw1, Huwe1, Kcmf1, Nedd4, Park7, Rnf14, Trim32, Ube3a, Ubr3, Ubr4, Ubr5, and STIP1 homology and U box-containing protein 1 (Stub1). In addition, other proteins pulled down by the ACR are components of E3 protein ligase complexes as follows: Cullin-4a (Cul4a); Cullin-4b (Cul4b); DNA damage-binding protein 1 (Ddb1); DDB1- and CUL4-associated factors 5 (Dcaf5) and 8 (Dcaf8); F-box only proteins 3 (Fbxo3) and 21 (Fbxo21); F-box/LRR-repeat protein 16 (Fbxl16); and Cereblon (Crbn). Cullins provide a scaffold for E3 ubiquitin ligases and combine with RING proteins to form Cullin-RING ubiquitin ligases (CRLs). Ddb1 primarily functions as a core component of the Cul4a- and Cul4b-based E3 ubiquitin ligase complexes (CRL4, E3 cullin 4-RING ligase) and serves as an adaptor protein that interacts with Dcaf class of proteins (74, 75). Dcafs are substrate specificity receptors that form the substrate-presenting side of the CRL4 complex (74, 75). Three of the proteins isolated are Dcaf: Dcaf5, Dcaf8, and Crbn. F-box proteins, such as Fbxo21, Fbxo3, and Fbxl16, are substrate recognition components of SCF (SKP1-CUL1-F-box protein) E3 ubiquitin ligase complex (76, 77).

The E3 ubiquitin-protein ligase activity of CRL complexes is dependent on the neddylation of the cullin subunit and is inhibited by the association of the deneddylated cullin subunit with the Cullin-associated NEDD8-dissociated protein 1 (TIP120A/CAND1) (78). CRL deneddylation is performed by the COP9 signalosome complex, a protein complex with isopeptidase activity that catalyzes the hydrolysis of NEDD8 protein from the cullins (79). Cand1 and all eight subunits composing the COP9 signalosomes (Cops1/2/3/4/5/6/7a/7b/8) were isolated in our ST-ACR pulldown experiments.

Proteasomes are ATP-dependent proteolytic complexes that degrade poly-ubiquitinated cytosolic and nuclear proteins. The proteasome most exclusively used in mammals is the cytosolic 26S proteasome (80). We found the following components of the proteasome among the potential ACR interactors: 26S protease regulatory subunit 4 (Psmc1); 6B (Psmc4); 8 (Psmc5); 10B (Psmc6); 26S proteasome non-ATPase regulatory subunits-1 (Psmd1); -2 (Psmd2); -4 (Psmd4); -7 (Psmd7); -8 (Psmd8); -11 (Psmd11); -12 (Psmd12); -13 (Psmd13); and -14 (Psmd14).

TABLE 1

E1, E2, and E3 interacting with the ACR, Ddb1, Crbn, Stub1, Cul4a, and Cul4b, are the most abundant UPS-linked proteins that bind to the ACR

Table contains the list of proteins identified (1st column); the database accession numbers (2nd column); the molecular mass in kDa (3rd column); and the NSAF (4th to 8th columns. Phosphorylation of Thr^{668} and/or Tyr^{682} does not significantly alter binding of these five proteins.

Proteins	UniProtKB/Swiss-Prot	kDa	St	ACR	$ACR^{Tyr(P)Thr(P)}$	$ACR^{Tyr(P)}$	$ACR^{Thr(P)}$
E1/E2							
Uba1	Q02053	118	0	0	0	0	0.0001
Ube2o	Q6ZPJ3	141	0	0	0.0001	0.0001	0.0003
Ube2r2	Q6ZWZ2	27	0	0.0005	0	0	0
E3							
Arih1	Q9Z1K5	64	0	0.0005	0	0.0002	0.0001
Hecw1	Q8K4P8	179	0	0	0	0	0.0001
Huwe1	Q7TMY8	483	0	0	0	0	0.0001
Kcmf1	Q80UY2	42	0	0.0002	0	0	0.0004
Nedd4	P46935	103	0	0.0003	0	0.0001	0
Park7	Q99LX0	20	0	0.0004	0	0.0005	0.0004
Rnf14	Q9JI90	55	0	0.0002	0	0	0
Trim32	Q8CH72	72	0	0.0008	0.0002	0.0011	0
Ube3a	O08759	101	0	0	0	0	0.0001
Ubr3	Q5U430	213	0	0.0001	0	0	0
Ubr4	A2AN08	572	0.0002	0.0010	0.0007	0.0005	0.0012
Ubr5	Q80TP3	308	0	0	0	0.0001	0.0001
Stub1	Q9WUD1	35	0	0.0093	0.0072	0.0055	0.0046
Cul4a	Q3TCH7	88	0	0.0015	0.0030	0.0009	0.0019
Cul4b	A2A432	111	0	0.0003	0.0009	0.0004	0.0007
Ddb1	Q3U1J4	127	0.0019	0.0141	0.0228	0.0114	0.0149
Dcaf5	Q80T85	104	0	0.0004	0	0.0001	0
Dcaf8	Q8N7N5	66	0	0.0002	0	0.0003	0
Fbxo3	Q9DC63	55	0	0.0002	0	0	0
Fbxo21	Q8VDH1	72	0	0.0001	0.0003	0.0001	0
Fbxl16	A2RT62	52	0	0.0006	0	0	0
Crbn	Q8C7D2	51	0	0.0061	0.0129	0.0053	0.0061

TABLE 2

Other UPS-related proteins interacting with the ACR

Table is organized same as Table 1. Binding of Pin1 and Grb2 (bottom two entries) is dependent on phosphorylation of Thr^{668} and Tyr^{682}, respectively.

	UniProtKB/Swiss-Prot	kDa	St	ACR	$ACR^{Tyr(P)Thr(P)}$	$ACR^{Tyr(P)}$	$ACR^{Thr(P)}$
E3 regulators							
Cand1	Q6ZQ38	136	0	0	0	0.0001	0
Cops1	Q99LD4	53	0	0.0007	0	0	0.0002
Cops2	P61202	52	0	0.0011	0	0.0002	0.0002
Cops3	O88543	48	0	0.0008	0	0	0
Cops4	O88544	46	0	0.0018	0	0	0.0002
Cops5	O35864	38	0	0.0013	0	0	0.0002
Cops6	O88545	36	0	0.0011	0	0.0002	0
Cops7a	Q9CZ04	30	0	0.0007	0	0	0
Cops7b	Q8BV13	30	0	0.0003	0	0	0
Cops8	Q8VBV7	23	0	0.0004	0	0	0
Proteasome							
Psmc1	P62192	49	0	0	0	0.0003	0
Psmc4	P54775	47	0	0	0	0.0003	0.0003
Psmc5	P62196	46	0	0.0003	0	0.0005	0.0006
Psmc6	P62334	44	0	0	0	0.0004	0
Psmd1	Q3TXS7	106	0	0	0	0.0001	0.0001
Psmd2	Q8VDM4	100	0	0.0001	0	0.0003	0.0001
Psmd4	O35226	41	0	0.0002	0.0003	0	0.0003
Psmd7	P26516	37	0	0	0	0.0002	0
Psmd8	Q9CX56	40	0	0.0002	0.0003	0	0.0002
Psmd11	Q8BG32	47	0	0	0	0.0002	0.0003
Psmd12	Q9D8W5	53	0	0.0002	0	0.0003	0.0002
Psmd13	Q9WVJ2	43	0	0	0	0.0002	0.0002
Psmd14	O35593	35	0	0	0	0.0002	0.0002
DUBs							
Usp9x	P70398	291	0	0.0005	0.0001	0.0003	0.0003
Usp5	P56399	96	0	0.0013	0.0003	0.0002	0.0003
Usp7	Q6A4J8	128	0	0.0002	0	0.0001	0.0001
Usp10	P52479	87	0	0.0001	0	0	0
Otub1	Q7TQI3	31	0	0.0008	0	0.0004	0.0004
Ubiquilins							
Ubqln1	Q8R317	62	0	0	0	0.0004	0
Ubqln2	UBQL2	67	0	0.0003	0.0006	0.0007	0.0003
Ubqln4	Q99NB8	64	0	0	0	0.0003	0
Phosphorylation-dependent							
Grb2	Q60631	25	0.0007	0.0008	0.0753	0.0350	0.0005
Pin1	Q9QUR7	18	0	0	0.0057	0	0.0030

Deubiquitinating enzymes (DUBs) are a large group of proteases that cleave ubiquitin from proteins and other molecules. Ubiquitination of a protein can have several biological consequences as follows: target the protein for degradation via the proteasome and autophagosome/lysosome; coordinate the cellular localization of proteins; activate and inactivate proteins; and modulate protein-protein interactions. DUBs can reverse these effects by cleaving off ubiquitin from substrate protein. In humans there are nearly 100 DUB genes, which can be classified into two main classes, cysteine proteases and metalloproteases (81). The cysteine proteases include many types of proteases, including ubiquitin-specific proteases and ovarian tumor proteases. Among the ACR-interacting proteins, we found five ubiquitin-specific proteases and one out: ubiquitin carboxyl-terminal hydrolase-9x (Usp9x); -5 (Usp5); -7 (Usp7); -10 (Usp10); and ubiquitin thioesterase Otub1.

Ubiquilins contain an NH_2-terminal ubiquitin-like domain and a COOH-terminal ubiquitin-associated domain. They physically associate with both proteasomes and ubiquitin ligases and thus are thought to functionally link the ubiquitination machinery to the proteasome (82). Three ubiquilins were isolated in our screening as follows: ubiquilin-1 (Ubqln1), -2 (Ubqln2), and -4 (Ubqln4).

$CRL4^{CRBN}$ E3 Ligase Complex and the E3 Ligase Stub1 Bind the COOH- and NH_2-terminal Regions of the ACR, Respectively—The UPS/ACR-interacting network is presumably formed via the direct interaction of the ACR with one or more UPS-linked proteins, and the other proteins are most likely indirectly associated with the ACR, for example via secondary interactions (*i.e.* mediated by binding to a direct ACR interactor) or tertiary interactions (*i.e.* mediated by binding to a protein that binds a direct ACR interactor) and so forth. It is reasonable to suppose that proteins binding to the ACR directly will be enriched more efficiently than proteins that bind indirectly. Normalized spectral abundance factor (NSAF) analysis indicates that Stub1, Ddb1, Crbn, Cul4a, and Cul4b are the five most abundant UPS-related proteins present in the St-ACR, St-$ACR^{Thr(P)}$, St-$ACR^{Tyr(P)}$, and St-$ACR^{Thr(P)Tyr(P)}$ pulldowns (Table 1; NSAF values for St-negative control, St-ACR, St-$ACR^{Thr(P)}$, St-$ACR^{Tyr(P)}$, and St-$ACR^{Thr(P)Tyr(P)}$ pulldowns were as follows: for Ddb1, 0.0019, 0.0141, 0.0228, 0.0114, and 0.0149; for Cul4a, 0, 0.0015, 0.003, 0.0009, and 0.0019; for Cul4b, 0, 0.0003, 0.0009, 0.0004, and 0.0007; for Crbn, 0, 0.0061, 0.0129, 0.0053, and 0.0061; and for Stub1, 0, 0.0091, 0.0072, 0.0055, and 0.0046). This quantitative analysis suggests that Stub1, Ddb1, Crbn, Cul4a, and Cul4b are the most likely UPS-related proteins to directly interact with APP and that phosphorylation of the ACR on either Thr^{668} or Tyr^{682} does not appreciably alter their binding to the ACR.

As a further step toward discriminating biologically relevant interactions from background noise, we used the above proteomic approach to identify the brain proteins interacting with the NH_2 terminus (JCasp) and COOH terminus (Ccas) subdomains of the ACR (Fig. 1*A*, *schematic*). In this experiment as well we used five baits as follows: the negative control St peptide, St-Ccas, St-Ccas with phosphorylation on Tyr^{682} (St-$Ccas^{Tyr(P)}$), St-Ccas with phosphorylation on Thr^{668} (St-$Ccas^{Thr(P)}$), and St-JCasp.

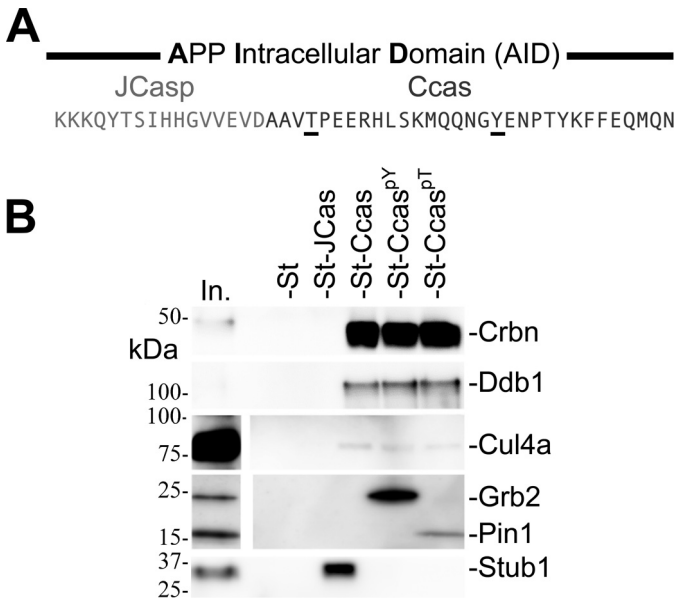

FIGURE 1. **Stub1 and $CRL4^{CRBN}$ E3 ligases bind distinct regions of the ACR.** *A,* schematic diagrams of the structural domains of the ACR. Jcasp and Ccas are generated by a double γ-secretase and caspase cleavage of APP. The Thr^{668} and Tyr^{682} residues that are phosphorylated are *underlined*. *B,* Western blotting analysis of pulldowns shows that Crbn, Ddb1, Cul4a, specifically bind St-Ccas, St-$Ccas^{Tyr(P)}$, and St-$Ccas^{Thr(P)}$. Stub1 binds specifically St-JCasp. Two previously known APP interactors, Grb2 and Pin1, bind St-$Ccas^{Tyr(P)}$ and St-$Ccas^{Thr(P)}$, respectively. This evidence validates the proteomic approach used. *In.* indicates the input. The WB shown are representative of at least three independent experiments.

JCasp and Ccas are two naturally occurring fragments that are generated by a double γ-secretase/caspase cleavage of APP (19–24); thus it is conceivable that this proteolytic event separates two functionally distinct intracellular regions of APP. Consistent with this thought, we found that Cul4a, Cul4b, Ddb1, Crbn, and Stub1 bind to distinct domains of the ACR (Table 3). Stub1 was the most abundant UPS-linked protein found in the St-JCasp pulldown and did not bind to St-Ccas peptides (NSAF for Stub1-derived peptides was 0, 0, 0, 0, and 0.0213 in St negative control, St-$Ccas^{Thr(P)}$, St-$Ccas^{Tyr(P)}$, St-Ccas, and St-JCasp pulldowns, respectively). Cul4a, Cul4b, Ddb1, and Crbn were the four most abundant UPS-linked proteins interacting with Ccas; their binding was not affected by phosphorylation, and they did not bind St-JCasp (NSAF for St negative control, St-$Ccas^{Thr(P)}$, St-$Ccas^{Tyr(P)}$, St-Ccas, and St-JCasp pulldowns were as follows: for Ddb1, 0.0005, 0.0478, 0.0273, 0.0375, and 0.0001; for Cul4a, 0, 0.0047, 0.003, 0.0026, and 0; for Cul4b, 0, 0.0011, 0.0006, 0.0008, and 0; for Crbn, 0, 0.0252, 0.0167, 0.0213, and 0). As noted above, Cul4a- or Cul4b-Ddb1 and Crbn form the $CRL4^{CRBN}$ E3 ligase complex; the evidence that all the $CRL4^{CRBN}$ E3 ligase complex components bind to the same domain of the ACR, Ccas, further supports the idea that they bind as a complex and not independently.

To confirm the accuracy of the proteins detected in the proteomic analysis, we performed Western blotting analysis with pulldown lysates. As shown in Fig. 1*B*, Crbn, Cul4a, and Ddb1 were readily detected in St-$Ccas^{Thr(P)}$, St-$Ccas^{Tyr(P)}$, and St-Ccas but not in St and St-JCasp pulldowns. On the contrary, Stub1 was found exclusively in St-JCasp pulldowns. Grb2, whose interaction with APP requires phosphorylation of Tyr^{682}

TABLE 3

Ddb1, Crbn, Cul4a, and Cul4b bind to Ccas and Stub1 binds to JCasp

Phosphorylation of Thr^{668} and/or Tyr^{682} does not significantly alter binding of Ddb1, Crbn, Cul4a, and Cul4b, whereas binding of Pin1 and Grb2 is dependent on phosphorylation of Thr^{668} and Tyr^{682}, respectively. Several of the other UPS-related proteins that are bound to the ACR bind to either Ccas or JCasp or both.

	UniProtKB/Swiss-Prot	Molecular mass	St	$Ccas^{Thr(P)}$	$Ccas^{Tyr(P)}$	Ccas	JCasp
		kDa					
E1 and E2							
Uba1	Q02053	118	0	0	0	0	0.0001
Ube2o	Q6ZPJ3	141	0	0	0	0	0.0001
Ube2r2	Q6ZWZ2	27	0	0	0	0	0.0016
E3							
Arih1	Q9Z1K5	64	0	0	0	0	0.001
Nedd4	P46935	103	0	0	0	0	0.0003
Park7	Q99LX0	20	0.0012	0.0017	0.0004	0.0022	0.002
Ubr4	A2AN08	572	0	0	0	0	0.0002
Stub1	Q9WUD1	35	0	0	0	0.0004	0.0213
Cul4a	Q3TCH7	88	0	0.0047	0.003	0.0026	0
Cul4b	A2A432	111	0	0.0011	0.0006	0.0008	0
Ddb1	Q3U1J4	127	0.0005	0.0478	0.0273	0.0375	0.0012
Crbn	Q8C7D2	51	0	0.0252	0.0167	0.0213	0
E3 regulators							
Cand1	Q6ZQ38	136	0.0002	0	0	0	0.0001
Cops1	Q99LD4	53	0	0	0	0	0.0018
Cops2	P61202	52	0	0	0	0	0.0022
Cops3	O88543	48	0	0	0	0	0.001
Cops4	O88544	46	0	0	0	0.0003	0.0024
Cops5	O35864	38	0	0	0	0	0.0011
Cops6	O88545	36	0	0	0	0	0.0015
Cops7a	Q9CZ04	30	0	0	0	0	0.0022
Cops7b	Q8BV13	30	0	0	0	0	0.0004
Cops8	Q8VBV7	23	0	0	0	0	0.0005
DUB							
Usp5	P56399	96	0	0.0001	0	0.0001	0.0019
Otub1	Q7TQI3	31	0	0.0004	0	0.0004	0.0007
Proteasome							
Psmd11	Q8BG32	47	0.0005	0	0	0.0003	0
Psmd12	Q9D8W5	53	0	0.0004	0	0.0002	0
Psmd13	Q9WVJ2	43	0	0	0	0.0003	0
Ubiquilin							
Ubqln2	Q9QZM0	67	0	0.0002	0.0001	0.0005	0.0002
Phosphorylation-dependent							
Grb2	Q60631	25	0.0062	0.0008	0.178	0.0005	0
Pin1	Q9QUR7	18	0	0.0126	0	0	0

(55, 59, 83), and Pin1, which interacts with APP in a Thr^{668} phosphorylation-dependent manner (84), were only detected in St-$Ccas^{Tyr(P)}$ and St-$Ccas^{Thr(P)}$ pulldowns, respectively, further validating the proteomic strategy.

Overall, the data suggest that of all the UPS-linked proteins pulled down with St-ACR, the $CRL4^{CRBN}$ E3 ligase complex components and E3 ligase Stub1 are the most likely to interact directly with APP *in vivo*. Incidentally, an interaction between Stub1 and APP *in vivo* was previously described (85). $CRL4^{CRBN}$ E3 ligase complex subunits and Stub1 bind to two distinct and non-overlapping domains of the APP intracellular domain: the NH_2-terminal JCasp for the E3 ligase Stub1 and the COOH-terminal Ccas regions for the components of the $CRL4^{CRBN}$ E3 ligase complex. Thus, it is conceivable that these two E3 ligases may interact with APP simultaneously.

Crbn Mediates Binding of the $CRL4^{CRBN}$ E3 Ligase Complex to the ACR—Next, we investigated whether Ddb1, Cul4, and Crbn interact with the ACR as a complex. Ddb1 and Cul4a bind several substrate-recognition subunits, called Dcaf. Indeed, Crbn is essentially a Dcaf. If the ACR interacted with the $CRL4^{CRBN}$ E3 ligase complex either via Cul4a, Cul4b, or Ddb1, several Dcafs should have been isolated by St-ACR. However, Crbn was the only Dcaf abundantly present in the pulldown with the four St-ACR baits (St-ACR, St-$ACR^{Thr(P)}$, St-$ACR^{Tyr(P)}$, and St-$ACR^{Thr(P)Tyr(P)}$) and the three St-Ccas baits (St-Ccas, St-$Ccas^{Thr(P)}$, and St-$Ccas^{Tyr(P)}$); Dcaf5 and Dcaf8 were detected but in very low amounts and only in St-ACR and St-$ACR^{Tyr(P)}$ pulldowns (NSAF for Dcaf5-derived peptides was 0.0004 and 0.0001 in St-ACR and St-$ACR^{Tyr(P)}$ pulldowns, respectively; NSAF for Dcaf8-derived peptides was 0.0002 and 0.0003 in St-ACR and St-$ACR^{Tyr(P)}$ pulldowns, respectively) and not in St-$ACR^{Thr(P)}$, St-$ACR^{Thr(P)Tyr(P)}$, St-Ccas, $Ccas^{Thr(P)}$, and St-$Ccas^{Tyr(P)}$ pulldowns (NSAF were 0 for both proteins in all five samples). Altogether, these data suggest that Dcaf5 and Dcaf8 may either have been non-specifically isolated in the St-ACR and St-$ACR^{Tyr(P)}$ pulldown or that Dcaf5 and Dcaf8 can weakly and indirectly interact with the ACR.

To directly test whether Crbn mediates the interaction of $CRL4^{CRBN}$ with APP, we performed St-$ACR^{Thr(P)Tyr(P)}$ pulldowns using brain lysates isolated either from wild type (WT) or *Crbn*-KO mice (86). Both proteomic (Table 4) and Western blotting analysis (Fig. 2) of these pulldowns show St-ACR binds Ddb1 and Cul4 when challenged with brain lysates isolated from WT mice but not when the brain lysates were derived from *Crbn*-KO (86) animals, albeit Ddb1 and Cul4 were equally

TABLE 4

Binding of Ddb1, Cul4a, and Cul4b to ACR$^{Thr(P)Tyr(P)}$ requires Crbn

Table contains the list of proteins identified (1st column); the database accession numbers (2nd column); the molecular mass in kDa (3rd column); NSAF of pulldown from WT mouse brains (4th column); NSAF of pulldown from *Crbn*-KO mouse brains (5th column). Binding of Stub1, Grb2, and Pin1 is independent of Crbn.

Proteins	UniProtKB/Swiss-Prot	Molecular mass	WT	*Crbn*-KO
		kDa		
Stub1	Q9WUD1	35	0.001	0.002
Ddb1	Q3U1J4	127	0.006	0
Crbn	Q8C7D2	51	0.004	0
Cul4a	Q3TCH7	88	0.001	0
Grb2	Q60631	25	0.013	0.018
Pin1	Q9QUR7	18	0.003	0.004

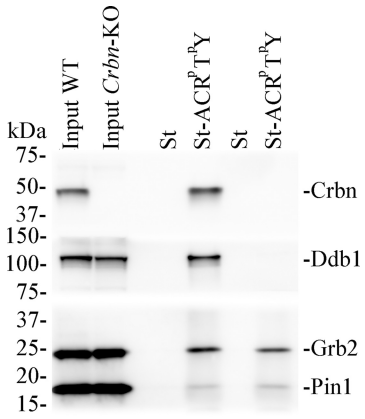

FIGURE 2. **Crbn mediates the interaction of CRL4^{CRBN} with APP.** Western blotting analysis shows that with St and St-ACR$^{Thr(P)Tyr(P)}$ binds Ddb1 only when Crbn in present in brain lysates, indicating that Crbn mediates the binding of CRL4^{CRBN} to the ACR. Binding of Grb2 and Pin1 to St-ACR$^{Thr(P)Tyr(P)}$ is not dependent on Crbn. The WB shown is representative of 4 independent experiments.

expressed in both WT and *Crbn*-KO lysates (Fig. 2). These data strongly suggest that Cul4, Ddb1, and Crbn bind to the ACR as a complex and that the APP cytoplasmic tail binds CRL4^{CRBN} via Crbn. On the contrary and as predictable, Stub1 (Table 4), Grb2, and Pin1 (Table 4 and Fig. 2) bind to St-ACR$^{Thr(P)Tyr(P)}$ independently of Crbn.

COOH Terminus of APP Binds the Substrate Recognition Pocket of Crbn—Although Thr^{668} and Tyr^{682} are in the Ccas ACR domain, phosphorylation of these residues does not modulate binding of CRL4^{CRBN} suggesting that they are not involved in the CRL4^{CRBN}-APP interaction. To further confirm this, we performed pulldowns with NH_2-terminal Ccas deletions and found that the COOH-terminal 12 amino acids of APP (St-C-12, which do non include Thr^{668} and Tyr^{682}) retain full binding capabilities for CRL4^{CRBN}, whereas the COOH-terminal eight amino acids (St-C-8) do not (Fig. 3*A*). Next, we performed pulldowns using a series of COOH-terminal deletions of St-C-12. Removal of the last one and two amino acids of APP reduces the binding of Crbn and Ddb1 by ~50 and ~100%, respectively. Essentially, when the NH_2-terminal amino acids of the 12-mer are deleted, binding was greatly reduced, as in the case with deleting the COOH-terminal two amino acids. It is therefore possible that reducing the ACR peptide below the length of 12 amino acids disrupts the peptide's secondary structure, thereby reducing Crbn and Ddb1 binding. Overall, the data indicate that the COOH-terminal 12 amino acids of APP contain the docking site for CRL4^{CRBN}.

Crbn is the substrate recognition subunit of CRL4^{CRBN} (49). To test whether APP binds the substrate-recognition pocket of Crbn, we pre-incubated brain lysates with either 10 or 100 μM concentrations of either thalidomide (Thal) or lenalidomide (Len), two compounds that bind the substrate-recognition pocket of Crbn (87–89). After 1 h, lysates were used for pulldown experiments with St-Ccas$^{Tyr(P)}$. Both thalidomide and lenalidomide reduced binding of Crbn and Ddb1 to St-Ccas$^{Tyr(P)}$ in a dose-dependent manner (Fig. 3*C*). Lenalidomide, which binds Crbn more efficiently than thalidomide, is more effective. As expected, neither thalidomide nor lenalidomide interfered with binding of Grb2 to St-Ccas$^{Tyr(P)}$ (Fig. 3*C*). In summary, the extreme COOH terminus of the ACR interacts with brain-derived CRL4^{CRBN} via the substrate-binding pocket of Crbn (model shown in Fig. 3*D*), suggesting that APP may be a substrate of the CRL4^{CRBN} E3 ligase.

APLP2, but not APLP1, Bind Stub1 and CRL4^{CRBN}—The APP protein family includes two other members, APLP1 and APLP2. These three proteins are functionally redundant, particularly APP and APLP2 (25, 45, 47, 90). APLP1 and APLP2 cytoplasmic regions (named AL1CR and AL2CR, respectively) are similar to that of APP. The ACR and the AL2CR share 66% identity and 16% similarity; the ACR and AL1CR share 53% identity and 21% similarity; and the AL2CR and the AL1CR share 62% identity and 18% similarity (Fig. 4*A*). As a first step toward determining whether APLP1 and/or APLP2 may functionally interface with UPS-related proteins, we characterized the brain interactome of the AL1CR and the AL2CR. We synthesized the control St-only peptides, St-AL1CR and St-AL2CR. As shown in Table 5, St-AL2CR interacts with Cul4a, Ddb1, and Crbn (see also Fig. 4*B*); Stub1 and three other E3 ubiquitin-protein ligases found in the ACR pulldown were Nedd4, Arih1, and Ubr4. As was the case for St-ACR pulldowns, Ddb1, Crbn, Stub1 and Cul4a were the four most abundant UPS-related proteins found in the St-AL2CR pulldown. In contrast, UPS-related proteins were scarcely represented in AL1CR pulldowns.

The COOH terminus of the ACR is essential for binding CRL4^{CRBN}; the AL2CR binds CRL4^{CRBN}, but the AL1CR does not; the COOH-terminal four amino acids of the ACR share 75 and 0% identity with the corresponding region of the AL2CR and AL1CR, respectively (Fig. 4*A*). These observations suggest that, like for the ACR, the COOH-terminal region of the AL2CR binds CRL4^{CRBN} via the substrate-binding pocket of Crbn. To test for this, we determined whether Crbn is required for binding of Ddb1 to the AL2CR. As shown in Fig. 4*C*, St-AL2CR binds Ddb1 when challenged with brain lysates isolated from WT animals but not when the input material is isolated from *Crbn*-KO mice. Next, we tested whether thalidomide and lenalidomide interfere with the AL2CR-Crbn interaction; indeed, both thalidomide and lenalidomide reduced binding of Crbn to St-AL2CR (Fig. 4*D*). Thus, like for the ACR, the AL2CR binds CRL4^{CRBN} via the substrate-binding pocket of Crbn. Overall, these data suggest that APP and APLP2, but not APLP1, may functionally interface with CRL4^{CRBN} and Stub1.

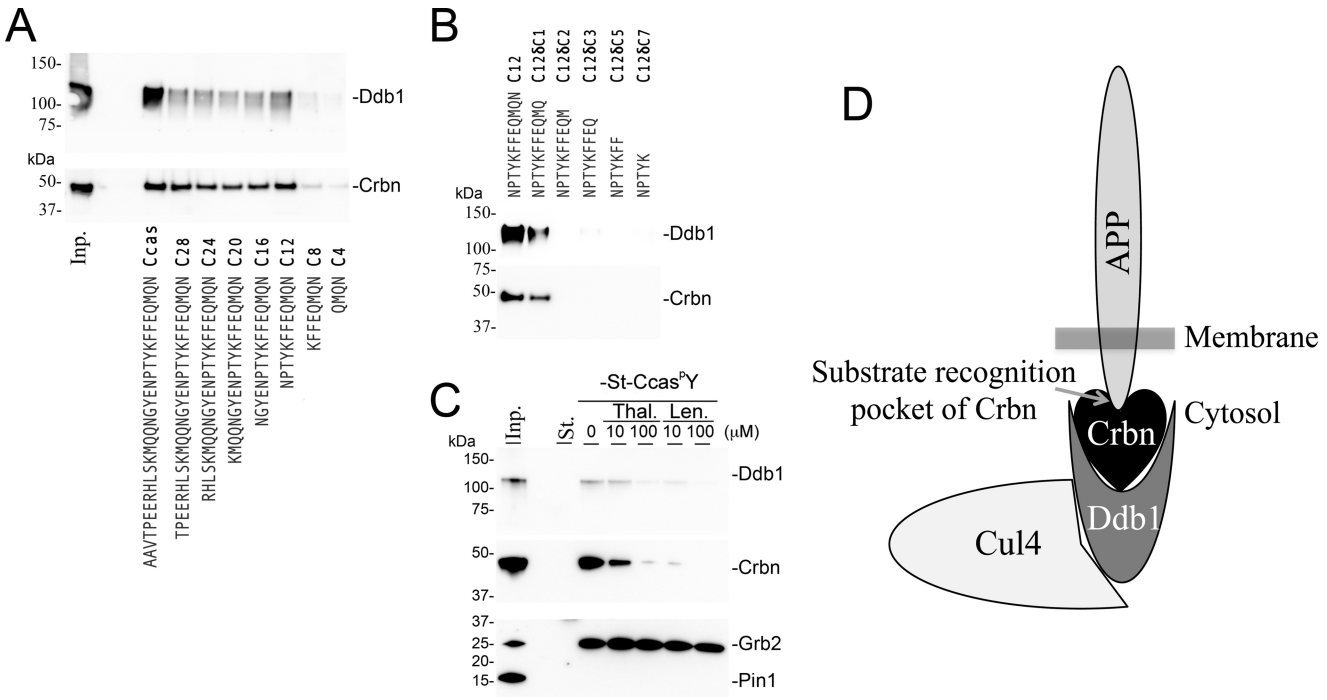

FIGURE 3. **APP-CRL4^{CRBN} complex is mediated by the interaction of the COOH terminus of APP with the substrate recognition pocket of Crbn.** *A,* sequences of the APP intracellular regions used as baits (St-Ccas, St-C28, St-C24, St-C20, St-C16, St-C12, St-C8, and St-C4) in the proteomic experiments are shown. Western blotting analysis of pulldowns with brains isolated from WT mice show that the COOH-terminal 12 amino acids of APP retain full binding activity to Crbn and Ddb1. The WB shown is representative of two independent experiments. *B,* sequences of the APP intracellular regions used as baits (St-C12, St-C12δC1, St-C12δC2, St-C12δC3, St-C12δC5, and St- St-C12δC7) in the proteomic experiments are shown. The WB shown is representative of two independent experiments. *C,* Western blotting analysis shows that thalidomide (*Thal.*) and lenalidomide (*Len.*), two compounds that bind to the substrate recognition pocket of Crbn, reduce binding of Crbn and Ddb1 from brain lysates to St-Ccas$^{Tyr(P)}$ in a dose-dependent manner. Thalidomide and lenalidomide do not interfere with binding of Grb2 to St-Ccas$^{Tyr(P)}$. Because Pin1 binding is dependent on phosphorylation of Thr^{668} of APP, Pin1 does not bind the St-Ccas$^{Tyr(P)}$ bait and is used as a negative control to show binding specificity. The WB shown is representative of three independent experiments. *D,* schematic model representing how Crbn mediated binding of CRL4^{CRBN} to the COOH terminus of APP, via its substrate recognition pocket.

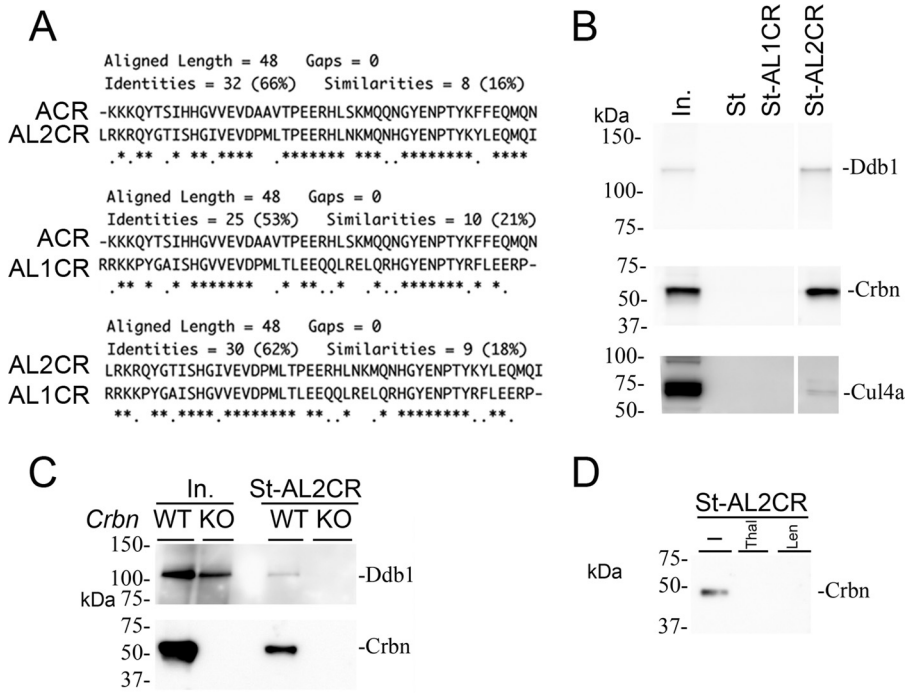

FIGURE 4. **AL2CR, but not the AL1CR, binds CRL4^{CRBN} via the substrate recognition pocket of Crbn.** *A,* alignments of the ACR, AL1CR, and AL2CR show that the ACR and the AL2CR are the most conserved intracellular regions of the APP protein family. *B,* Western blotting analysis of pulldowns with brains isolated from WT mice shows that the AL2CR, but not the AL1CR, interacts with Cul4a, Ddb1, and Crbn. The WB shown is representative of two independent experiments. *C,* St-AL2CR binds Ddb1 in lysate from WT but not from *Crbn*-KO mice. The WB shown is representative of three independent experiments. *D,* Western blotting analysis of St-AL2CR pulldowns from brains isolated from WT mice shows that incubation of the lysates with either thalidomide and lenalidomide prior to pulldowns interferes with the AL2CR-Crbn interaction. The WB shown is representative of two independent experiments.

ACR and the AL2CR Pull Down Active E3 Ubiquitin-Protein Ligase(s)—Ubiquitination of proteins is a multistep reaction. First, an E1 ubiquitin-activating enzyme activates ubiquitin. Next, ubiquitin is transferred on one of many ubiquitin-conjugating enzyme (E2s). The E2 is loaded on an E3 ubiquitin-protein ligase, which directs the mono- and poly-ubiquitination of substrate proteins. The presence of many of these components in St-ACR and St-AL2CR pulldowns prompted us to test whether ubiquitinating activity could be detected. To this end, we performed an *in vitro* ubiquitination assay using FLAG-ubiquitin as an external source of ubiquitin. The reactions were analyzed by Western blotting using an α-FLAG antibody to determine whether the FLAG-ubiquitin (~9 kDa) was incorporated into larger complexes. A smear of FLAG-ubiquitinated proteins was clearly detected in the St-ACR and St-AL2CR pulldowns after supplemental addition of recombinant E2 UbcH5a/UBE2D1 (Fig. 5*A*). Overimposed on the smear was a ladder of bands starting at ~25 kDa, which are ~9 kDa apart (Fig. 5*A*). The ~25-kDa band is compatible with mono-ubiquitinated recombinant E2; the higher bands likely represent recombinant E2 linked to a progressively increasing number of ubiquitin molecules. Addition of recombinant E1 Ube1, albeit not necessary, further potentiated the ubiquitination reactions (Fig. 5*A*). The observation that only recombinant E2 is required to initiate ubiquitination activity (Fig. 5*A*) indicates that St-ACR and St-AL2CR bring down from the mouse brain functional E1 and E3 ubiquitin-protein ligase(s). Of note, neither the smear nor the ladder was visible in the *in vitro* ubiquitination assay of St and St-AL1CR eluates (Fig. 5*A*), further stressing that APP and APLP2, but not APLP1, may functionally interface with the ubiquitination system.

Because active E3 ubiquitin-protein ligases undergo auto-ubiquitination, we tested whether Crbn was ubiquitinated *in vitro*. The St-ACR *in vitro* ubiquitination assay was analyzed by Western blotting with an α-Crbn antibody; in addition to full-length Crbn, a ladder of signals compatible with Crbn molecules linked to an increasing number of ubiquitins was detected (Fig. 5*B*). This evidence suggests that St-ACR interacts with an active brain-derived $CRL4^{CRBN}$ complex.

ACR Facilitates Ubiquitination of ACR-interacting Proteins in Vitro—The smear detected by the α-FLAG antibody hints at ubiquitination of numerous proteins. To test this hypothesis, we performed another *in vitro* ubiquitination assay on St-$ACR^{Thr(P)Tyr(P)}$ pulldown because it includes proteins that interact with APP in a $Thr(P)^{668}$- and $Tyr(P)^{682}$-dependent manner. The reaction was immunoprecipitated with the α-FLAG M2-agarose beads, and proteins were eluted from the M2-agarose beads using a competing 3×FLAG peptide. To identify the lysine residues ubiquitinated (K-ub) *in vitro*, the eluted material was subjected to the ubiquitin remnant motif (K-ε-GG) assay (UbiScan). In parallel, we performed UbiScan experiments on total mouse brain lysates to determine whether K-ubs found in the *in vitro* assay are also ubiquitinated *in vivo*. In addition, we used as further reference the Cell Signaling Data Bank collection of UbiScan results from rodent, human, and chicken tissue, which can be found on line.

As reported in Table 6, several brain-derived proteins associated with the ACR bait were ubiquitinated. These proteins can be separated into four groups as follows: (*a*) group 1, proteins of the ubiquitin-conjugating system; (*b*) group 2, presynaptic proteins; (*c*) group 3, other proteins implicated in AD; and (*d*) group 4, phosphorylation-dependent ACR interactors.

Group 1: consistent with the Western blot showing ubiquitination of Crbn (Fig. 5*B*), we found six K-ub from Crbn, four of which have been found *in vivo*. Two other components of

TABLE 5

UPS-related proteins, including Ddb1, Crbn, Stub1, Cul4a, and Cul4b, bind to the AL2CR but not to the AL1CR

The table contains the list of proteins identified (1st column); the database accession numbers (2nd column); the molecular mass in kDa (3rd column); NSAF of pulldown of WT mouse brains with St alone (4th column); St-AL1CR (5th column); and NSAF of pulldown of WT mouse brains with St-AL2CR (6th column).

Proteins	UniProtKB/ Swiss-Prot	Molecular mass	St	AL1CR	AL2CR
		kDa			
Ddb1	Q3U1J4	127	0.0021	0.0014	0.0356
Crbn	Q8C7D2	51	0	0	0.01810
Stub1	Q9WUD1	35	0	0	0.01427
Cul4a	Q3TCH7	88	0	0	0.00310
E3 Nedd4	P46935	103	0	0	0.00264
Otub1	Q7TQI3	31	0	0	0.00244
Usp5	P56399	96	0	0.0007	0.00189
Uba1	Q02053	118	0	0	0.00103
Cops4	O88544	46	0	0	0.00099
Fbxl16	A2RT62	52	0	0	0.00058
Fbxo3	Q9DC63	55	0	0	0.00055
E3 Arih1	Q9Z1K5	64	0	0	0.00047
Dcaf8	Q8N7N5	66	0	0	0.00046
Ubqln2	Q9QZM0	67	0	0	0.00045
E3 Ubr4	A2AN08	572	0	0	0.00024
Usp9x	P70398	291	0	0	0.00021

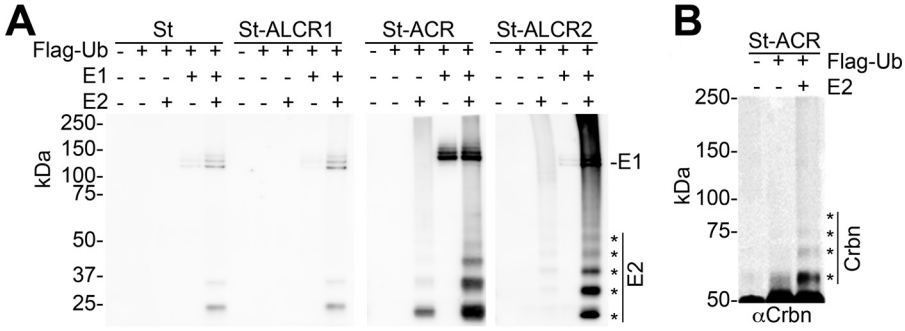

FIGURE 5. **ACR and the AL2CR bind an active $CRL4^{CRBN}$.** *A,* St, St-ACR, St-AL1CR, and St-AL2CR mouse brain pulldowns were incubated with (+) or without (−) ubiquitin-FLAG (*Ub-FLAG*), E2, and/or E1. After the reaction, these *in vitro* ubiquitination assays were probed on WB with an anti-FLAG antibody. E2 promotes ubiquitination in St-ACR and St-AL2CR pulldowns. The WB shown is representative of five independent experiments. *B,* WB with an α-CRBN antibody indicates the *in vitro* ubiquitination assays of St-ACR brain pulldowns where Crbn is poly-ubiquitinated, indicating that St-ACR isolates from brain an active $CRL4^{CRBN}$. The WB shown is representative of two independent experiments.

TABLE 6

***In vitro* ubiquitination of proteins present in the St-ACR$^{Tyr(P)Thr(P)}$ pulldowns**

1st column lists some of the proteins ubiquitinated *in vitro* in an ACR$^{Tyr(P)Thr(P)}$-dependent manner. 2nd column lists all the lysine residues found ubiquitinated *in vitro*. The K-ub found in our UbiScans from mouse brains are indicated with (m*) and in previous UbiScan experiments from mouse (m), human (h), rat (r) and chicken (c) tissues, which are reported online. 3rd column reports database accession numbers.

Ubiquitin conjugating system		
Cul4a	8, 23, h33, 42, 46, 65, 71, 97, m/h104, 133, 134, 191, 330, 404, 411, 416, m465, 473, 708, 724, 728, 734, 749	Q3TCH7
Cul4b	m112, 247, m315, 398, 460, 495, m676, 684, 931, 939	A2A432
Crbn	h/c46, h119, h/m303, 395, 410, c416	Q8C7D2
Chip	126	Q9WUD1
Arih1	457	Q9Z1K5
Mib2	344, 369, 426, 435	Q8R516–2
Nedd4	m*445, m/h453	P46935
Cbl-b	37, m*491, h516, 615	Q3TTA7
Ube3a	28	O08759
Ube1	m/h802	Q02053
Ube2n	m/h/r82, m/h/r92, m/h/r94	P61089
Ube2o	m/h812, m/h816	Q6ZPJ3
Presynaptic proteins		
Scamp1	h/m/r334	Q8K021
Sv2a	m*32	Q9JIS5
Sv2b	m*62, m65, m341	Q8BG39
Vamp2	m/h/r52, m/h/r59, m/h83, m*/h/r85	P63044
Atp6v0a1	m262, m/h295	Q9Z1G4
Vglu1	m283	Q3TXX4
Syt1	r98, m/r104, m*190, r196, m200, m369	P46096
Syt2	m*191	P46097
Rab14	m/h/r193	Q91V41
Rab3a	m12	P63011
Snap-25	m/r103	P60879
Syn2	280	Q64332
Syn1	m256, m281, r299, m311, m593	O88935
Notable targets		
ApoE	m105	P08226
Tau	m*455, m*613	P1063
Phosphorylation-dependent interactors		
Grb2	h69, m*/h76	Q60631
Pin1	h/r65, 97, h99, m/h119, h134	Q9QUR7

CRL4^{CRBN} were ubiquitinated (23 K-ub for Cul4a and 10 K-ub for Cul4b, six of which have been found *in vivo*). Other E3 ubiquitin-protein ligases ubiquitinated are as follows: Stub1 (Lys^{126}, new), Arih1 (Lys^{457}, new), Mib2 (Lys^{344}, Lys^{426}, Lys^{435}, new, and Lys^{369} known), Nedd4 (Lys^{445}, found in our mouse brain UbiScan; Lys^{453}, previously found *in vivo*), Cbl-b (Lys^{37} and Lys^{615}, new; Lys^{491}, found in our mouse brain UbiScan; Lys^{516}, previously found *in vivo*), Ube3a (Lys^{28}, new). Finally, brain-derived E1 Ube1 and E2s Ube2n and Ube2o (which is actually an E2/E3 hybrid ubiquitin-protein ligase) were also ubiquitinated: all these ubiquitinations have been found *in vivo*.

Group 2: in this group are included the following single-pass and multi-pass synaptic vesicle membrane proteins (Fig. 6): the vesicular SNARE Vamp2; the Ca^{2+}-sensors synaptotagmin-1 and -2 (Syt1 and Syt2); the secretory carrier-associated membrane protein 1 Scamp1; the synaptic vesicle glycoproteins Sv2a and Sv2b; the vesicular glutamate transporter Vglu1, and Atp6v0a1 that is required for assembly and activity of the vacuolar ATPase. All these K-ub are found *in vivo*. Moreover, these ubiquitinated lysine residues are all localized in the cytosolic domains (Fig. 6); this is relevant because in physiological conditions only lysine residues exposed to the vesicular lumen are not available to the ubiquitination system, suggesting that the *in vivo* ubiquitination of these two lysines is plausible. Other proteins associated with synaptic vesicles, such as the trans-SNARE Snap25, Synapsin2 and Synapsin1 (Syn1/2), and the G proteins Rab3a and Rab14, were ubiquitinated *in vitro* on lysine residues that, with the exception of Lys^{280} of Syn2, are also ubiquitinated *in vivo*.

Ubiquitination of these presynaptic proteins is not entirely surprising. Indeed, the interaction of the ACR with Syt1, Syt2, Sv2a, Sv2b, Snap-25, and Vamp2 was reported previously (28). Moreover, two other studies have shown that APP interacts *in vivo* with Syn1, Syt1, Vamp2, Syn2, Sv2a, Snap-25, and Rab3A (91, 92). In Table 7, we show proteomic data substantiating the association of the ACR with Scamp1, Atp6v0a1, Vglu1, Rab14, Rab3a, Syn2, and Syn1.

Group 3: this group includes the tubulin-binding protein Tau (93) and the cholesterol transporter apoE (94). Both proteins were detected in St-ACR pulldowns (Table 7). The two Tau K-ubs found *in vitro* (Lys^{455} and Lys^{613}) were also identified in our mouse brain UbiScan. It is worth noting that Stub1 can mediate Tau ubiquitination (95, 96) suggesting that the ACR may facilitate Tau ubiquitination via interaction with Stub1 on one side and Tau on the other side. Alternatively, the ACR may interact with Tau indirectly, via Stub1. It is worth noting that a previous study has described a physical interaction between APP and Tau *in vivo* (97). ApoE was ubiquitinated on Lys^{105}. ApoE is a secreted protein and its ubiquitination may be an *in vitro* artifact. However, ubiquitination of Lys^{105} of apoE has been reported *in vivo*, suggesting that apoE is, at least in a small fraction or in certain conditions, resident in the cytosol. Indeed, previous work has shown that apoE is cleaved by a neuro-specific chymotrypsin-like serine protease that generates bioactive

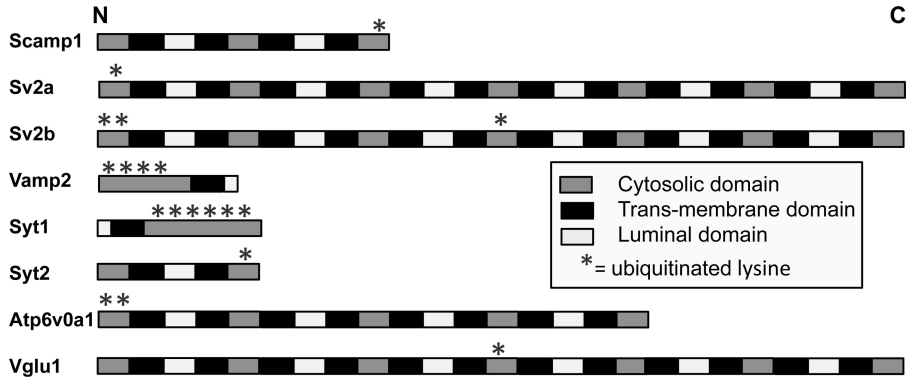

FIGURE 6. **Only lysine residues present in cytosolic domains of transmembrane proteins are ubiquitinated *in vitro*.** Schematic representation of single pass and multipass transmembrane presynaptic vesicle proteins that interact with the ACR and are ubiquitinated *in vitro* in an ACR-dependent manner. Notably, all the lysine residues ubiquitinated *in vitro* are in segments that are exposed to the cytosol.

TABLE 7

Proteins ubiquitinated *in vitro* (see Table 6) interact with the ACR

Table lists the proteins identified (1st column); the molecular mass in kDa (2nd column); NSAF (4th to 8th columns). Here we show the proteomic data documenting the interaction of Vglu1, Atp6v0a1, Scamp1, Rab14, Rab3a, Syn2, Syn1, ApoE, and Tau with the ACR.

Proteins	kDa	St	ACR	$ACR^{Tyr(P)Thr(P)}$	$ACR^{Tyr(P)}$	$ACR^{Thr(P)}$
Vglu1	62	0	0.0013	0.0015	0.0004	0.0031
Atp6v0a1	96	0	0.0012	0.0014	0.0003	0.0024
Scamp1	38	0	0.0002	0	0	0.0003
Rab14	24	0	0.0025	0.0030	0.0036	0.0035
Rab3a	25	0	0.0019	0.0024	0.0028	0.0025
Syn2	63	0	0.0016	0.0017	0.0011	0.0008
Syn1	74	0	0.0023	0.0042	0.0023	0.0022
ApoE	36	0	0.0020	0.0039	0.0030	0.0033
Tau	76	0	0.0010	0.0006	0.0004	0.0012

intraneuronal truncated forms of apoE (98, 99) and that apoE is ubiquitinated in cell lines (100).

Group 4: we also found two Grb2 K-ubs and five Pin1 K-ubs. All of these K-ubs are found *in vivo*. This evidence suggests that phosphorylation of APP on Thr^{668} and Tyr^{682} could potentially alter the function of proteins that bind APP in a phosphorylation-dependent manner by regulating their ubiquitination.

Although it is doubtful that all the ACR-dependent ubiquitinations detected in this *in vitro* assay are physiologically relevant, the data suggest that APP may work as a substrate recognition subunit of one or more E3 ubiquitin-protein ligases (possible candidates are $CRL4^{CRBN}$ and Stub1), and APP may regulate ubiquitination of some of the proteins described here.

In Vitro Ubiquitination of the ACR-interacting Proteins Occurs on a Subset of the Lysine Residues Ubiquitinated in Vivo—Next, we compared the *in vitro* UbiScan with the UbiScan performed in parallel on mouse brain lysates. We found that only few of the lysine residues ubiquitinated in the brain were also ubiquitinated *in vitro*. A few examples are shown in Table 8. Only one lysine residue of Scamp1, Sv2a, SNAP-25, and apoE was ubiquitinated *in vitro*. In contrast, additional K-ubs (six for Scamp1 and -3 for Sv2a and four for apoE) were detected in mouse brains. Syt1 and Tau were ubiquitinated on 19 and 16 lysine residues in mouse brains, respectively; of these, only five and two lysine residues were ubiquitinated *in vitro*, respectively. This evidence suggests the following. 1) APP may facilitate ubiquitination of a subset of "ubiquitinable" lysine residues on potential substrates and as a result APP could fine-tune the function of substrates with high accuracy by targeting lysine residues residing in specific functional domains. 2) Additional lysine residues of putative APP substrates are presumably ubiquitinated by distinct E3 ligases, possibly with distinct functional outcomes. 3) The stability of potential APP substrates can be regulated by APP-dependent and APP-independent mechanisms.

ACR Is Ubiquitinated in Vitro, Evidence for a Role of $CRL4^{CRBN}$ in Ubiquitination of Lys^{676} of the ACR—As expected, recombinant E1 and E2 were ubiquitinated *in vitro* (data not shown). Interestingly, we also found ubiquitination of synthetic ACR on Lys^{649}, Lys^{650}, Lys^{651}, Lys^{676}, and Lys ^{688} (see Table 9). Ubiquitination of Lys^{651}, Lys^{676}, and Lys^{688} was also found in normal tissues, including our mouse brain UbiScan, whereas ubiquitination of Lys^{649} and Lys^{650} has been reported in cell lines (101). These data suggest that E3 ubiquitin-protein ligases present in the pulldown may be responsible for APP ubiquitination *in vivo*.

To test the role of $CRL4^{CRBN}$ in ubiquitination of the ACR, we performed an *in vitro* ubiquitination assay of the ACR pulldowns from either WT or *Crbn*-KO mouse brains followed by UbiScan analysis. As shown in Table 9, ubiquitination of Lys^{676} was significantly reduced in pulldowns from *Crbn*-KO brains; in contrast, ubiquitination of Lys^{649}, Lys^{650}, Lys^{651}, and Lys^{688} was similar in both WT- and *Crbn*-KO-derived samples. Together these data suggest the following. 1) $CRL4^{CRBN}$ E3 ubiquitin-protein ligase, which is absent in pulldown from *Crbn*-KO brains, may have a primary, perhaps not exclusive, role in ubiquitination of APP on Lys^{676}. 2) Other E3 ubiquitin-protein ligases participate in ubiquitination of residues Lys^{649}, Lys^{650}, Lys^{651}, and Lys^{688}.

Discussion

In this study, we provide *in vitro* evidence suggesting that APP may function as a substrate recognition unit for one or more E3 ubiquitin-protein ligases. This hypothesis is supported by the following findings. 1) The cluster of brain proteins that may interact with APP via the ACR is rich in proteins that regulate the UPS (Table 1). 2) The E3 ubiquitin-protein ligases $CRL4^{CRBN}$ and Stub1 are the most abundant UPS-related proteins interacting with the ACR (Tables 1 and 3 and Fig. 1*B*). 3) The E3 ubiquitin-protein ligase interacting with the ACR is enzymatically active and ubiquitinates the five lysine residues

TABLE 8

In vitro* ubiquitination of ACR-interacting proteins occurs on a subset of the lysine residues ubiquitinated *in vivo

The 1st column lists some of the proteins ubiquitinated *in vitro* in an ACR-dependent manner. The 2nd column reports all the lysine residues found ubiquitinated in the mouse brain lysate UbiScan that we performed (*in vivo* ubiquitinations). The 3rd column reports the lysine residues found ubiquitinated in our *in vitro* ubiquitination/UbiScan experiment.

Protein	K-ub found in our UbiScans from mouse brains	K-ub found in the *in vitro* ubiquitination/UbiScan assay of ACR^{pTpY}-pulldown
Scamp1	52, 65, 78, 89, 298, 311, 334	334
Sv2a	32, 143, 375, 398	32
Syt1	98, 104, 107, 189, 190, 191, 200, 213, 267, 272, 288, 297, 321, 332, 366, 369, 420, 421	98, 104, 190, 200, 369
SNAP-25	40, 96, 102, 103, 184, 189, 201	103
ApoE	85, 86, 105, 173, 252	105
Tau	455, 546, 551, 566, 603, 609, 613, 623, 632, 635, 645, 661, 662, 667, 677, 730	455, 613

TABLE 9

E3 ligases interacting with the ACR ubiquitinate the five lysine residues of the ACR

The 1st column shows the site of modification for the peptide assignment. The 2nd column reports the amino acid sequence for the peptide assignment with the ubiquitinated lysine (*). The 3rd column reports the relative fold-change between the integrated peak area of the experimental (numerator, *Crbn*-KO) and control (denominator, WT) conditions. A negative value indicates the peptide is more abundant in the control condition.

Site	Peptide	Normalized fold change *Crbn*-KO/WT
649	K*KKQYTSIHHGVVEVDAAVTPEER	1.4
650	KK*KQYTSIHHGVVEVDAAVTPEER	1.3
651	KK*QYTSIHHGVVEVDAAVTPEER	1.4
676	HLSK*MQQNGYENPTYK	−3.9
688	MQQNGYENPTYK*FFEQMQN	−1.2

TABLE 10

Ubiquitination of Lys^{676} is significantly reduced in the absence of $CRL4^{CRBN}$

Table shows the parent ion intensity observed during the MS at its chromatographic apex for the two WT samples (1st and 2nd columns) and the two *Crbn*-KO samples (3rd and 4th columns).

Normalized intensity			
WT (1)	WT (2)	*Crbn*-KO (1)	*Crbn*-KO (2)
5,690,496	6,303,560	9,363,865	9,691,813
429,867	688,670	835,455	739,774
1,480,860	1,749,112	2,392,320	2,704,107
6,532,470	6,297,230	1,840,820	1,776,503
37,117,469	32,761,543	38,646,971	26,595,257

present in the APP cytoplasmic region (Fig. 5*A* and Table 5). 4) The APP cytosolic domain facilitates ubiquitination of interacting proteins *in vitro* (Table 6).

The five cytoplasmic APP residues (Lys^{649}, Lys^{650}, Lys^{651}, Lys^{676}, and Lys^{688}), which are ubiquitinated *in vivo*, are also ubiquitinated *in vitro* in ACR pulldowns (Table 9) suggesting that the E3 ubiquitin-protein ligase(s) present in the pulldown interaction may be responsible for ubiquitination of APP *in vivo*. The evidence that ubiquitination of Lys^{676}, but not that of the other four ACR lysine residues, is significantly reduced in the absence of $CRL4^{CRBN}$ (Table 10) suggests the following: 1) Lys^{676} of APP may be physiologically ubiquitinated mainly, but not exclusively, by the $CRL4^{CRBN}$ E3 ubiquitin-protein ligase; 2) Lys^{649}, Lys^{650}, Lys^{651}, and Lys^{688} are probably targets of other E3 ubiquitin-protein ligases, although a role for $CRL4^{CRBN}$ cannot be formally excluded, like Stub1 that is very abundant in the ACR pulldown. Because the subunits of $CRL4^{CRBN}$ undergo auto-ubiquitination (Table 6 and Fig. 5*B*), the possibility that APP may at the same time act as a substrate recognition unit and a substrate of a $CRL4^{CRBN/APP}$ E3 ubiquitin-protein ligase is not far-fetched.

APP belongs to a protein family that includes APLP1 and APLP2. Analysis of single and double knock-out (KO and dKO) mice has shown that *App*-KO, *Aplp1*-KO, *Aplp2*-KO, and *App/Aplp1*-dKO have minor deficits. In contrast, *App/Aplp2*-dKO mice have severe neuromuscular junctions deficits, are significantly smaller than *App*-KO and *Aplp2*-KO mice, and die within the first 28 days of life (25, 43, 102, 103). These data indicate that APP and APLP2 share some essential function that cannot be compensated for by APLP1. However, the molecular mechanisms mediating this essential function (or functions) of APP and APLP2 are unclear. Here, we show that the brain interactomes of the ACR and the AL2CR, but not of the AL1CR, share many UPS-related proteins, including Stub1 and $CRL4^{CRBN}$ (Table 5 and Fig. 4*B*). Moreover, the AL2CR interacts, like the ACR, with the substrate recognition pocket of Crbn (Fig. 4, *C* and *D*). Finally, the ACR and the AL2CR brain interactomes possess E3 ubiquitin-protein ligase activity, whereas the brain interactome of the AL1CR does not (Fig. 5*A*). Altogether, these data suggest that both APP and APLP2 may possess E3 ubiquitin-protein ligase substrate recognition activity, which is not compensated for by APLP1. Thus, the loss of this activity may mechanistically cause the severe phenotype of *App/Aplp2*-dKO mice.

APP facilitates glutamatergic transmitter release, likely through the interaction with the neurotransmitter release machinery (28). In addition, the APP intracellular domain has been linked to many other pathological and functional pathways, including caspase activation, transcription, Ca^{2+} flux, and neurodegeneration (28, 31, 32, 34, 40, 46, 64, 104, 106–108). It is tempting to speculate that APP may affect all these seemingly unrelated pathways via a single mechanism of action. Indeed, by acting as a substrate recognition unit for E3 ubiquitin-protein ligase(s), APP could modulate ubiquitination of proteins involved in these processes (model in Fig. 7). Thus, using a single modus operandi, APP may regulate disparate and apparently unrelated signaling pathways. As we show here, many of the proteins that control synaptic vesicle functions and interact with APP are ubiquitinated *in vitro* in an ACR-dependent manner (Table 6). Consequently, APP may aid synaptic vesicle activity by modulating ubiquitination of these proteins, thereby altering their stability and/or their function.

Eleven UPS-linked proteins isolated by St-ACR and five brain-derived proteins that are ubiquitinated *in vitro* in an ACR-dependent manner are associated with genetic diseases of the central nervous system and neuromuscular system. These include *HUWE1*, *CRBN*, *CUL4B*, *USP9X*, *PARK7*, *STUB1*,

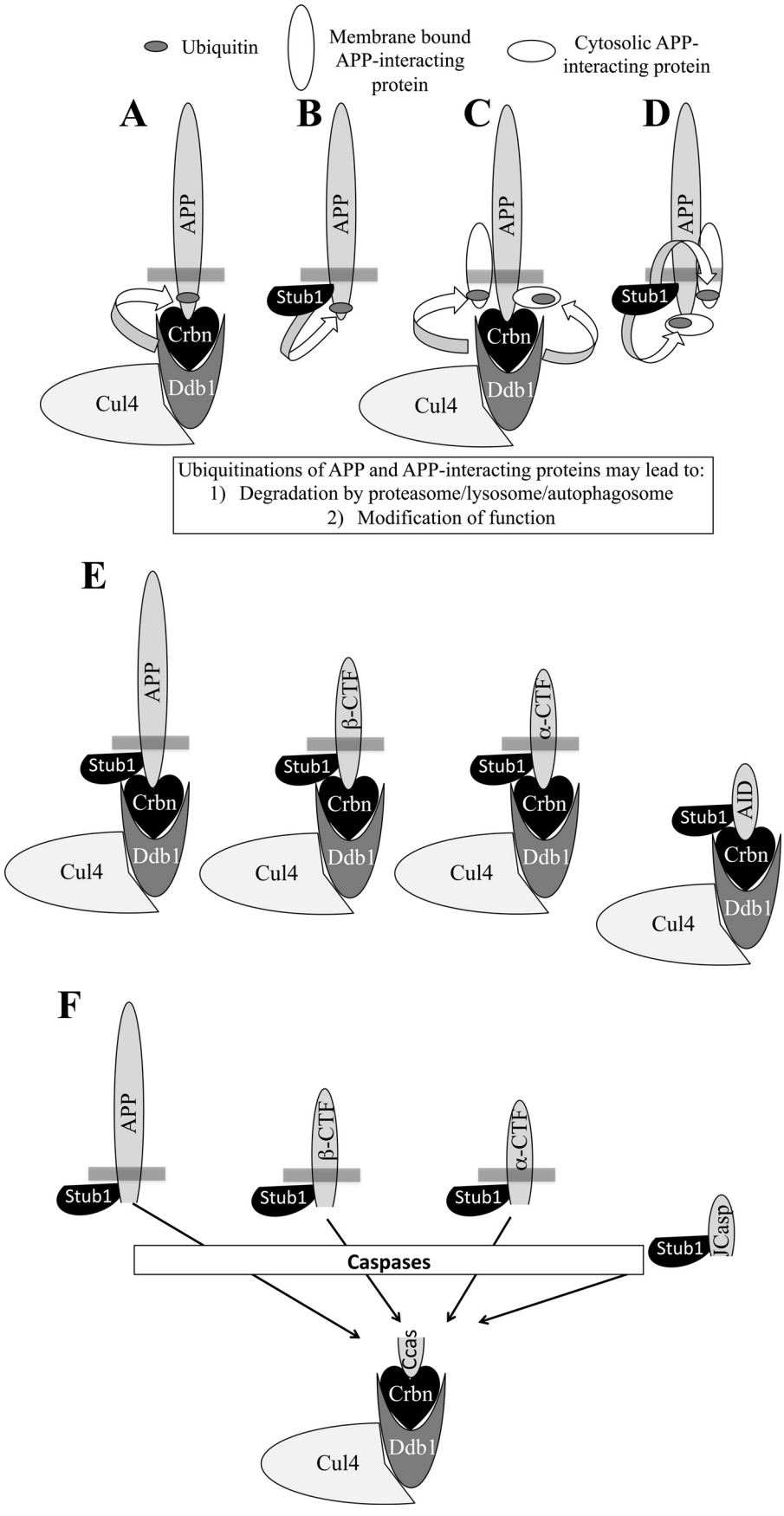
Ubiquitin
Membrane bound APP-interacting protein
Cytosolic APP-interacting protein
A
B
C
D
APP
Stub1
Crbn
Ddb1
Cul4
Ubiquitinations of APP and APP-interacting proteins may lead to:
1) Degradation by proteasome/lysosome/autophagosome
2) Modification of function
E
β-CTF
α-CTF
AID
F
Caspases
JCasp
Ccas

DCAF8, *TRI32*, *UBE3A*, *UBQL2*, *UBA1*, *SYT2*, *SNAP-25*, *SYN1*, *APOE,* and *TAU* (109–139).

These observations suggest a molecular and functional connection between APP and other proteins genetically involved in Alzheimer and other neurodegenerative diseases. Tau is the main component of neuronal tangles that characterize AD, and *TAU* mutations are linked to genetic forms of frontotemporal dementia. Previous studies have shown that APP and Tau interact *in vivo* (97). Interestingly, Stub1 mediates ubiquitination of Tau, and Tau is polyubiquitinated at several sites in AD patients (140–142). Thus, a role of APP in Tau ubiquitination would be both biologically and pathologically significant. *APOE* is the main genetic risk factor for sporadic AD, with the *APOE4* allele increasing the risk of developing late onset AD (137). Our *in vitro* evidence suggesting that APP may both interact with and regulate ubiquitination of apoE is inciting and needs to be developed further. Four of the proteins discussed in this study (HUWE1, CRBN, CUL4B, and USP9X) are genetically linked to intellectual disability (previously known as mental retardation). Remarkably, this list includes two $CRL4^{CRBN}$ E3 ubiquitin-protein ligase components, CRBN and CUL4A. Overall, these data suggest a functional network that comprises many proteins that, when functionally altered by genetic mutations, trigger neurodegenerative disorders. Hence, it is reasonable to speculate that dysregulation of this functional network, in which APP as a modulator of E3 ubiquitin-protein ligase(s) may play a crucial role, could be a pathogenic mechanism shared by numerous neuronal disorders. This concept is not outlandish because accumulation of ubiquitinated protein inclusions in neurodegenerative diseases and the link between mutations in proteins involved in the UPS and neurodegenerative disorders are both established truths (52, 105, 143).

Several APP-derived metabolites contain the ACR and can interact with Stub1 and $CRL4^{CRBN}$ (Fig. 7*E*). These include the following: 1) full-length APP; 2) β-CTF and α-CTF, which are the products of β- and α-secretase cleavage of full-length APP; and 3) AID/AICD peptide, which is produced by γ-secretase cleavage of β-CTF and α-CTF. Like full-length APP, β-CTF and α-CTF are membrane-bound; in principle, full-length APP-Stub1/$CRL4^{CRBN}$, β-CTF-Stub1/$CRL4^{CRBN}$, and α-CTF-Stub1/$CRL4^{CRBN}$ complexes could have distinct functions, although this concept may not be immediately obvious. In contrast, processing of β-CTF and α-CTF by γ-secretase would release AID-Stub1/$CRL4^{CRBN}$ complexes from membranes. This may have several predictable biological consequences, including a down-modulation of the APP-dependent ubiquitination of trans-membrane proteins.

Stub1 and $CRL4^{CRBN}$ could contemporarily bind to the ACR because they interact with the NH_2 and COOH termini of this APP region, respectively. Thus, cleavage of APP by caspases at Asp^{664} could functionally separate the activities linked to the APP-Stub1 and APP-$CRL4^{CRBN}$ complexes.

In future studies, it will be important to test these hypotheses, to determine whether pathogenic APP mutation regulate this function of APP and whether this deregulation has any pathogenic role in neurodegeneration.

Experimental Procedures

Mice and Ethics Statement—Mice were maintained on a C57BL/6 background for at least 15 generations. Mice were handled according to the Ethical Guidelines for Treatment of Laboratory Animals of Albert Einstein College of Medicine. The procedures were described and approved by the Institutional Animal Care and Use Committee (IACUC) at the Albert Einstein College of Medicine as animal protocol number 20130509.

Mouse Brain Preparation—Whole mouse brains were Dounce-homogenized (1:10 w/v) in 20 mM Tris base, pH 7.4, 250 mM sucrose, 1 mM EDTA, 1 mM EGTA supplemented with protease and phosphatase inhibitors (catalog no. 1861282, lot no. QH220492A, ThermoScientific). Brain homogenates were centrifuged at 800 × *g* for 10 min at 4 °C. Supernatant were collected and centrifuged at 9200 × *g* for 10 min at 4 °C to obtain the pellet (P2) and the supernatant (S2) fractions. The P2 fractions were resuspended in 5 mM Tris base, pH 7.4, 35.6 mM sucrose, 1 mM EDTA, 1 mM EGTA supplemented with protease and phosphatase inhibitors and lysed for 30 min at 4 °C rotating. Samples were centrifuged at 18,900 × *g* for 15 min at 4 °C. The supernatants were collected (LS1 fraction).

Strep-tag Peptide Synthesis—The following Strep-tag (St) peptides used for pulldown experiments were synthesized and purified by the Tufts University Core Facility (Boston, MA). The St sequence is underlined. The phosphorylated residues are indicated with a ^{P}: St, WSHPQFEK; St-ACR, WSHPQFEKGAVMLKKKQYTSIHHGVVEVDAAVTPEERHLSKMQQNGYENPTYKFFEQMQN; St-ACR^{pT}, WSHPQFEKGAVMLKKKQYTSIHHGVVEVDAAVTPEERHLSKMQQNG^{P}YENPTYKFFEQMQN; St-ACR^{pT}, WSHPQFEKGAVMLKKKQYTSIHHGVVEVDAAV^{P}TPEERHLSKMQQNGYENPTYKFFEQMQN; St-ACR^{pTpY}, WSHPQFEKGAVMLKKKQY^{P}TSIHHGVVEVDAAV^{P}TPEERHLSKMQQNG^{P}YENPTYKFFEQMQN; St-Ccas, WSHPQFEKAAVTPEERHLSKMQQNGYENPTYKFFEQMQN; St-$Ccas^{pY}$, WSHPQFEKAAVTPEERHLSKMQQNG^{P}YENPTYKFFEQMQN; St-$Ccas^{pT}$, WSHPQFEKAAV^{P}TP-

FIGURE 7. **APP could be both a substrate and a substrate recognition subunit of Stub1 and $CRL4^{CRBN}$ E3 protein ligases.** *A,* $CRL4^{CRBN}$ mediates ubiquitination of lysine residue(s) present in the cytoplasmic tail of APP (with Lys^{756} being the most likely candidate). *B,* Stub1 could also be involved in the ubiquitination of cytoplasmic APP lysine residue(s). *C,* APP could bridge cytosolic and membrane-bound proteins to $CRL4^{CRBN}$ *de facto* functioning as a substrate recognition unit of a $CRL4^{CRBN\text{-}APP}$ E3 ubiquitin-protein ligase. *D,* in this final model APP is postulated to act as a substrate recognition unit for a Stub1-APP E3 ubiquitin-protein ligase, mediating ubiquitination of cytosolic and/or membrane-bound proteins that interact with the ACR ubiquitination of APP, and APP-binding proteins could lead to functional modification and/or to degradation of the ubiquitinated proteins by the proteasome, autophagosomes, and/or lysosomes. *E,* some of the APP-derived metabolites that contain the ACR and can potentially interact with Stub1 and $CRL4^{CRBN}$. Processing of full-length APP by β-, α-, and γ-secretase can have several functional consequences. For example, it is possible that full-length APP-Stub1/$CRL4^{CRBN}$, β-CTF-Stub1/$CRL4^{CRBN}$, and α-CTF-Stub1/$CRL4^{CRBN}$ complexes have distinct functions, *i.e.* that the ectodomain of APP may influence the function of the ACR. That processing of β-CTF and α-CTF by γ-secretase could have functional consequences is obvious. Indeed, AID-Stub1/$CRL4^{CRBN}$ complexes are released from membranes. This may, among other things, result into down-modulation of the APP-dependent ubiquitination of trans-membrane proteins. *F,* cleavage of APP-Stub1/$CRL4^{CRBN}$, β-CTF-Stub1/$CRL4^{CRBN}$, α-CTF-Stub1/$CRL4^{CRBN}$, and AID-Stub1/$CRL4^{CRBN}$ by caspases could functionally separate the activities linked to the various ACR-Stub1 and ACR-$CRL4^{CRBN}$ complexes.

EERHLSKMQQNGYENPTYKFFEQMQ; St-JCasp, WSHPQFEKVMLKKKQYTSIHHGVVEVD; St-C4, WSHPQFEKQMQN; St-C8, WSHPQFEKKFFEQMQN; St-C12, WSHPQFEKNPTYKFFEQMQN; St-C16, WSHPQFEKNGYENPTYKFFEQMQN; St-C20, WSHPQFEKKMQQNGYENPTYKFFEQMQN; St-C24, WSHPQFEKRHLSKMQQNGYENPTYKFFEQMQN; St-C28, WSHPQFEKTPEERHLSKMQQNGYENPTYKFFEQMQN; St-C28δ2, WSHPQFEKTPEERHLSKMQQNGYENPTYKFFEQM; St-C28δ3, WSHPQFEKTPEERHLSKMQQNGYENPTYKFFEQ; St-C28δ5, WSHPQFEKTPEERHLSKMQQNGYENPTYKFF; St-C28δ7, WSHPQFEKTPEERHLSKMQQNGYENPTYK; St-AL1CR, WSHPQFEKRRKKPYGAISHGVVEVDPMLTLEEQQLRELQRHGYENPTYRFLEERP; and St-AL2CR, WSHPQFEKLRKRQYGTISHGIVEVDPMLTPEERHLNKMQNHGYENPTYKYLRQMQI.

Pulldown Assays with St-peptides—The St-peptides were immobilized on StrepTactin column (catalog no. 2-1209-550, IBA-GmbH, Goettingen, Germany). S2 plus LS1 brain fractions were pre-cleared on StrepTactin columns containing no St-peptides. Pre-cleared). Pre-cleared S2 plus LS1 brain fractions were next passed through the StrepTactin column loaded with St-peptides. The columns were then washed, and St-peptides, together with brain proteins specifically bound to the St-peptide, were eluted with desthiobiotin following the manufacturer's recommendations. In some pulldowns, brain lysates were incubated for 1 h at 4 °C with the indicated concentrations of either lenalidomide (catalog no. T2800, lot 2570277, LKT Laboratories, Inc., St. Paul, MN) or thalidomide (catalog no. 0652, batch 11A/141284, Tocris Bioscience, Bristol, UK), prior to pulldown with St-peptides.

In Vitro Ubiquitination Assay—Pulldown samples were incubated in 50 mM Tris, pH 7.6, 5 mM $MgCl_2$, 2 mM ATP, 0.6 mM DTT, with/without 40 ng of the E1 UBE1 (catalog no. E-305, lot 16114714, BostonBiochem, Cambridge, MA), 0.3 μg of the E2 UbcH5a/UBE2D1 (catalog no. E2-616, Lot 04201314C, BostonBiochem, Cambridge, MA), 1 μg of ubiquitin-FLAG (catalog no. U-211, Lot DBGI0215011, BostonBiochem), 1 μM recombinant human HA ubiquitin aldehyde, C terminus (catalog no. U-556, lot 0AB03101C, BostonBiochem). Reactions were incubated overnight at 30 °C. The final volume of the reaction was 30 μl/sample.

Immunoprecipitation of the in Vitro Ubiquitination Assays—To isolate proteins ubiquitinated *in vitro*, the *in vitro* ubiquitination assay performed on St-ACR pulldown was incubated with FLAG-M2 affinity gel (catalog no. A2220, lot SLBF8148, Sigma), under constant rotation for 3 h at 4 °C. The agarose beads were collected by centrifugation and washed five times in phosphate-buffered saline plus 0.05% Tween. After washing, the proteins bound to FLAG-M2 affinity gel were eluted by incubation with 100 μM concentration of the 3×FLAG competing peptide (catalog no. F4799, lot SLBG0131V, Sigma).

Mouse Brain Preparation for UbiScan—To process the brain tissue for UbiScan analysis, brains from at least eight animals of the same genotype for each experiment were cut into small pieces and lysed in freshly prepared urea lysis buffer (20 mM Hepes, 9 M urea, 1 mM sodium orthovanadate, 2.5 mM sodium pyrophosphate, 1 mM β-glycerol phosphate), using 4 ml of buffer for 100 mg of tissue. Samples were homogenized twice using a Polytron set to maximum speed, using 20-s-long pulses. Between pulses, samples were chilled on ice for 1 min. Successively, samples were sonicated using a microtip set to 15-watt output using three bursts of 30 s each. Between bursts, samples were chilled on ice for 1 min. Finally, the lysates were cleared from debris by centrifugation at 20,000 × *g* for 15 min at 4 °C.

UbiScan Analysis—This analysis was performed by the PTMScan Facility at Cell Signaling Technology. Briefly, samples were digested with trypsin; after digestion, peptides were loaded directly onto a 10 cm × 75 μm PicoFrit capillary column packed with Magic C18 AQ reversed-phase resin. The column was developed with a 90-min linear gradient of acetonitrile in 0.125% formic acid delivered at 280 nl/min. Ubiquitinated peptides were enriched by immunoprecipitation with the ubiquitin branch motif antibody (K-ε-GG) (catalog no. 3925). Samples were subjected to LC-MS/MS analysis using LTQ-Orbitrap-Velos, ESI-CID. MS parameter settings are as follows: MS run time of 96 min; MS1 scan range (300.0–1500.00); top 20 MS/MS (minimum signal 500; isolation width 2.0; normalized collision energy 35.0; activation-Q 0.250; activation time 20.0; lock mass 371.101237; charge state rejection enabled, charge state 1+ rejected; dynamic exclusion enabled, repeat count 1; repeat duration 35.0; exclusion list size 500; exclusion duration 40.0; exclusion mass width relative to mass; exclusion mass width 10 ppm). MS/MS spectra were evaluated using SEQUEST 3G and the CORE platform from Harvard University. Searches were performed against the most recent update of the NCBI *Mus musculus* database with mass accuracy of ±50 ppm for precursor ions and 1 Da for product ions. Results were filtered with mass accuracy of ±5 ppm on precursor ions and presence of the intended motif (K-ε-GG).

Western Blotting (WB) Analysis and Antibodies Specificity—Samples were separated on 4–20% SDS-PAGE (catalog no. 345-0125, Bio-Rad) and transferred onto nitrocellulose membranes (catalog no. 106000012, GE Healthcare). The following data presented here support the specificity of the antibodies as follows. (*a*) A band of the predicted size for Ddb1, Pin1, Stub-1, Grb2, Cul4a, and Crbn are detected both in total lysates and in pulldown samples. (*b*) These bands are visible only in pulldown samples in which Ddb1, Pin1, Stub-1, Grb2, Cul4a, and Crbn are detected by nano-LC/MS/MS. (*c*) Crbn is not detectable in samples derived from *Crbn*-KO brains. The following antibodies were used in WB: anti-Ddb1 (catalog no. 6998s, lot 1, rabbit monoclonal antibody, Cell Signaling Technology, dilution 1:300); anti-Pin-1 (catalog no. 3722s, lot 3, rabbit polyclonal antibody, Cell Signaling Technology, dilution 1:1000); anti-Stub1 (catalog no. 2080s, lot 2, rabbit polyclonal antibody, Cell Signaling Technology, dilution 1:300); anti-Grb2 (catalog no. 3972s, lot 2, rabbit polyclonal antibody, Cell Signaling Technology, dilution 1:1000); anti-Cul4a (catalog no. 14851-1-AP, lot 1, rabbit polyclonal antibody, ProteinTech, dilution 1:300); anti-Crbn (catalog no. HPA045910, lot Q103829, rabbit polyclonal antibody, Sigma, dilution 1:500); and anti-FLAG M2 (catalog no. A2220, lot SLBF8148, mouse monoclonal antibody, Sigma, dilution 1:1000). This antibody detects a signals-only in samples in which ubiquitin-FLAG and the ubiquitination machinery are present (Fig. 5*A*). Incubations with primary antibodies were performed in phosphate-buffered saline plus 0.05%

Tween 20 (catalog no. H5151, Promega) and 5% bovine serum albumin fraction V (BSA, catalog no. BP1605-100, lot 146598, Fisher) overnight in a cold room. We used the following HRP-conjugated secondary antibodies. For WB with mouse monoclonal primary antibodies, we used the goat anti-mouse HRP-conjugated antibody (catalog no. 1031-05, lot I0912-ML33B, Southern Biotech, dilution 1:1000). For WB with rabbit primary antibodies, we used two goat anti-mouse HRP-conjugated secondary antibodies (catalog no. 4050-05, lot E0513-ZF44, Southern Biotech, dilution 1:1000; catalog no. 7074, lot 25, Cell Signaling Technology, dilution 1:1000). Membranes were incubated with secondary antibodies in phosphate-buffered saline plus 0.05% Tween 20 and 5% Blotting-Grade blocker nonfat dry milk (catalog no. 170-6404, Bio-Rad), at room temperature for 1 h. After washing in phosphate-buffered saline plus 0.05% Tween, WB was developed using either SuperSignal West Dura stable peroxidase (catalog no. 34076, lot QL226061, Pierce) or SuperSignal West Pico stable peroxidase (catalog no. 1859674, lot OB182893, Pierce). Signals were acquired using ImageQuant LAS 4000 mini and ImageQuant LAS 4000 software (GE Healthcare).

Mass Spectrometry—MS Bioworks, LLC, Ann Arbor, MI, performed this analysis. The volume of each pulldown sample was reduced to 50 μl by vacuum centrifugation; 20 μl of each concentrated sample was processed by SDS-PAGE using a 10% BisTris NuPAGE gel (Invitrogen); with the MES buffer system the gel was run ~2 cm. The mobility region was excised into 10 equally sized segments, and in-gel digestion was performed on each using a robot (ProGest, DigiLab) with the following protocol: washing with 25 mM ammonium bicarbonate followed by acetonitrile; reduced with 10 mM dithiothreitol at 60 °C followed by alkylation with 50 mM iodoacetamide at room temperature; digested with trypsin (Promega) at 37 °C for 4 h; quenched with formic acid; and the supernatant was analyzed directly without further processing. Each digest was analyzed by nano-LC/MS/MS with a Waters NanoAcquity HPLC system interfaced to a ThermoFisher Q Exactive mass spectrometer. Peptides were loaded on a trapping column and eluted over a 75-μm analytical column at 350 nl/min; both columns were packed with Jupiter Proteo resin (Phenomenex). The mass spectrometer was operated in data-dependent mode, with MS and MS/MS performed in the Orbitrap at 70,000 and 17,500 full width at half-maximum resolution, respectively. The 15 most abundant ions were selected for MS/MS.

Author Contributions—L. D. conceived and coordinated the study and wrote the paper. D. D. P. and L. D. designed, performed, and analyzed all the experiments. D. D. P. contributed to writing the paper. A. M. R. provided reagents/knock-out mice and contributed to writing the paper. R. C. R. generated knock-out mice. L. D. and D. D. P. prepared the figures. L. D. prepared the tables. All authors reviewed the results and approved the final version of the manuscript.

References

1. Jonsson, T., Atwal, J. K., Steinberg, S., Snaedal, J., Jonsson, P. V., Bjornsson, S., Stefansson, H., Sulem, P., Gudbjartsson, D., Maloney, J., Hoyte, K., Gustafson, A., Liu, Y., Lu, Y., Bhangale, T., *et al.* (2012) A mutation in APP protects against Alzheimer's disease and age-related cognitive decline. *Nature* **488,** 96–99
2. Matsuda, S., Giliberto, L., Matsuda, Y., Davies, P., McGowan, E., Pickford, F., Ghiso, J., Frangione, B., and D'Adamio, L. (2005) The familial dementia BRI2 gene binds the Alzheimer gene amyloid-β precursor protein and inhibits amyloid-β production. *J. Biol. Chem.* **280,** 28912–28916
3. Egashira, N., Iwasaki, K., Takashima, A., Watanabe, T., Kawabe, H., Matsuda, T., Mishima, K., Chidori, S., Nishimura, R., and Fujiwara, M. (2005) Altered depression-related behavior and neurochemical changes in serotonergic neurons in mutant R406W human τ transgenic mice. *Brain Res.* **1059,** 7–12
4. Matsuda, S., Giliberto, L., Matsuda, Y., McGowan, E. M., and D'Adamio, L. (2008) BRI2 inhibits amyloid β-peptide precursor protein processing by interfering with the docking of secretases to the substrate. *J. Neurosci.* **28,** 8668–8676
5. Matsuda, S., Matsuda, Y., and D'Adamio, L. (2009) BRI3 inhibits amyloid precursor protein processing in a mechanistically distinct manner from its homologue dementia gene BRI2. *J. Biol. Chem.* **284,** 15815–15825
6. Tanzi, R. E. (2012) The genetics of Alzheimer disease. *Cold Spring Harb. Perspect. Med.* **2,** a0066296
7. Vidal, R., Frangione, B., Rostagno, A., Mead, S., Révész, T., Plant, G., and Ghiso, J. (1999) A stop-codon mutation in the BRI gene associated with familial British dementia. *Nature* **399,** 776–781
8. Garringer, H. J., Murrell, J., D'Adamio, L., Ghetti, B., and Vidal, R. (2010) Modeling familial British and Danish dementia. *Brain Struct. Funct.* **214,** 235–244
9. Vidal, R., Revesz, T., Rostagno, A., Kim, E., Holton, J. L., Bek, T., Bojsen-Møller, M., Braendgaard, H., Plant, G., Ghiso, J., and Frangione, B. (2000) A decamer duplication in the 3′ region of the BRI gene originates an amyloid peptide that is associated with dementia in a Danish kindred. *Proc. Natl. Acad. Sci. U.S.A.* **97,** 4920–4925
10. De Strooper, B. (2007) Loss-of-function presenilin mutations in Alzheimer disease. talking point on the role of presenilin mutations in Alzheimer disease. *EMBO Rep.* **8,** 141–146
11. De Strooper, B., Vassar, R., and Golde, T. (2010) The secretases: enzymes with therapeutic potential in Alzheimer disease. *Nat. Rev. Neurol.* **6,** 99–107
12. De Strooper, B., and Voet, T. (2012) Alzheimer's disease: a protective mutation. *Nature* **488,** 38–39
13. Baulac, S., LaVoie, M. J., Kimberly, W. T., Strahle, J., Wolfe, M. S., Selkoe, D. J., and Xia, W. (2003) Functional γ-secretase complex assembly in Golgi/trans-Golgi network: interactions among presenilin, nicastrin, Aph1, Pen-2, and γ-secretase substrates. *Neurobiol. Dis.* **14,** 194–204
14. Borchelt, D. R., Lee, M. K., Gonzales, V., Slunt, H. H., Ratovitski, T., Jenkins, N. A., Copeland, N. G., Price, D. L., and Sisodia, S. S. (2002) Accumulation of proteolytic fragments of mutant presenilin 1 and accelerated amyloid deposition are co-regulated in transgenic mice. *Neurobiol. Aging* **23,** 171–177
15. Bennett, B. D., Babu-Khan, S., Loeloff, R., Louis, J. C., Curran, E., Citron, M., and Vassar, R. (2000) Expression analysis of BACE2 in brain and peripheral tissues. *J. Biol. Chem.* **275,** 20647–20651
16. Annaert, W., Cupers, P., Saftig, P., and De Strooper, B. (2000) Presenilin function in APP processing. *Ann. N.Y. Acad. Sci.* **920,** 158–164
17. De Strooper, B. (2003) Aph-1, Pen-2, and nicastrin with presenilin generate an active γ-Secretase complex. *Neuron* **38,** 9–12
18. Pellegrini, L., Passer, B. J., Tabaton, M., Ganjei, J. K., and D'Adamio, L. (1999) Alternative, non-secretase processing of Alzheimer's β-amyloid precursor protein during apoptosis by caspase-6 and -8. *J. Biol. Chem.* **274,** 21011–21016
19. Gervais, F. G., Xu, D., Robertson, G. S., Vaillancourt, J. P., Zhu, Y., Huang, J., LeBlanc, A., Smith, D., Rigby, M., Shearman, M. S., Clarke, E. E., Zheng, H., Van Der Ploeg, L. H., Ruffolo, S. C., Thornberry, N. A., *et al.* (1999) Involvement of caspases in proteolytic cleavage of Alzheimer's amyloid-β precursor protein and amyloidogenic A β peptide formation. *Cell* **97,** 395–406
20. Weidemann, A., Paliga, K., Dürrwang, U., Reinhard, F. B., Schuckert, O., Evin, G., and Masters, C. L. (1999) Proteolytic processing of the Alzheimer's disease amyloid precursor protein within its cytoplasmic domain

by caspase-like proteases. *J. Biol. Chem.* **274,** 5823–5829
21. Passer, B. J., Pellegrini, L., Vito, P., Ganjei, J. K., and D'Adamio, L. (1999) Interaction of Alzheimer's presenilin-1 and presenilin-2 with Bcl-X(L). A potential role in modulating the threshold of cell death. *J. Biol. Chem.* **274,** 24007–24013
22. Lu, D. C., Rabizadeh, S., Chandra, S., Shayya, R. F., Ellerby, L. M., Ye, X., Salvesen, G. S., Koo, E. H., and Bredesen, D. E. (2000) A second cytotoxic proteolytic peptide derived from amyloid β-protein precursor. *Nat. Med.* **6,** 397–404
23. Madeira, A., Pommet, J. M., Prochiantz, A., and Allinquant, B. (2005) SET protein (TAF1β, I2PP2A) is involved in neuronal apoptosis induced by an amyloid precursor protein cytoplasmic subdomain. *FASEB J.* **19,** 1905–1907
24. Bertrand, E., Brouillet, E., Caillé, I., Bouillot, C., Cole, G. M., Prochiantz, A., and Allinquant, B. (2001) A short cytoplasmic domain of the amyloid precursor protein induces apoptosis *in vitro* and *in vivo*. *Mol. Cell. Neurosci.* **18,** 503–511
25. Barbagallo, A. P., Wang, Z., Zheng, H., and D'Adamio, L. (2011) A single tyrosine residue in the amyloid precursor protein intracellular domain is essential for developmental function. *J. Biol. Chem.* **286,** 8717–8721
26. Li, H., Wang, Z., Wang, B., Guo, Q., Dolios, G., Tabuchi, K., Hammer, R. E., Südhof, T. C., Wang, R., and Zheng, H. (2010) Genetic dissection of the amyloid precursor protein in developmental function and amyloid pathogenesis. *J. Biol. Chem.* **285,** 30598–30605
27. Barbagallo, A. P., Wang, Z., Zheng, H., and D'Adamio, L. (2011) The intracellular threonine of amyloid precursor protein that is essential for docking of Pin1 is dispensable for developmental function. *PLoS One* **6,** e18006
28. Fanutza, T., Del Prete, D., Ford, M. J., Castillo, P. E., and D'Adamio, L. (2015) APP and APLP2 interact with the synaptic release machinery and facilitate transmitter release at hippocampal synapses. *Elife* **4,** e09743
29. Klevanski, M., Herrmann, U., Weyer, S. W., Fol, R., Cartier, N., Wolfer, D. P., Caldwell, J. H., Korte, M., and Müller, U. C. (2015) The APP intracellular domain is required for normal synaptic morphology, synaptic plasticity, and hippocampus-dependent behavior. *J. Neurosci.* **35,** 16018–16033
30. Hamid, R., Kilger, E., Willem, M., Vassallo, N., Kostka, M., Bornhövd, C., Reichert, A. S., Kretzschmar, H. A., Haass, C., and Herms, J. (2007) Amyloid precursor protein intracellular domain modulates cellular calcium homeostasis and ATP content. *J. Neurochem.* **102,** 1264–1275
31. Passer, B., Pellegrini, L., Russo, C., Siegel, R. M., Lenardo, M. J., Schettini, G., Bachmann, M., Tabaton, M., and D'Adamio, L. (2000) Generation of an apoptotic intracellular peptide by γ-secretase cleavage of Alzheimer's amyloid β protein precursor. *J. Alzheimers Dis.* **2,** 289–301
32. Cao, X., and Südhof, T. C. (2001) A transcriptionally (correction of transcriptively) active complex of APP with Fe65 and histone acetyltransferase Tip60. *Science* **293,** 115–120
33. Cupers, P., Orlans, I., Craessaerts, K., Annaert, W., and De Strooper, B. (2001) The amyloid precursor protein (APP)-cytoplasmic fragment generated by γ-secretase is rapidly degraded but distributes partially in a nuclear fraction of neurones in culture. *J. Neurochem.* **78,** 1168–1178
34. Pardossi-Piquard, R., Petit, A., Kawarai, T., Sunyach, C., Alves da Costa, C., Vincent, B., Ring, S., D'Adamio, L., Shen, J., Müller, U., St George Hyslop, P., and Checler, F. (2005) Presenilin-dependent transcriptional control of the Aβ-degrading enzyme neprilysin by intracellular domains of βAPP and APLP. *Neuron* **46,** 541–554
35. Liu, Q., Zerbinatti, C. V., Zhang, J., Hoe, H. S., Wang, B., Cole, S. L., Herz, J., Muglia, L., and Bu, G. (2007) Amyloid precursor protein regulates brain apolipoprotein E and cholesterol metabolism through lipoprotein receptor LRP1. *Neuron* **56,** 66–78
36. von Rotz, R. C., Kohli, B. M., Bosset, J., Meier, M., Suzuki, T., Nitsch, R. M., and Konietzko, U. (2004) The APP intracellular domain forms nuclear multiprotein complexes and regulates the transcription of its own precursor. *J. Cell Sci.* **117,** 4435–4448
37. Kim, H. S., Kim, E. M., Lee, J. P., Park, C. H., Kim, S., Seo, J. H., Chang, K. A., Yu, E., Jeong, S. J., Chong, Y. H., and Suh, Y. H. (2003) C-terminal fragments of amyloid precursor protein exert neurotoxicity by inducing glycogen synthase kinase-3β expression. *FASEB J.* **17,** 1951–1953
38. Baek, S. H., Ohgi, K. A., Rose, D. W., Koo, E. H., Glass, C. K., and Rosenfeld, M. G. (2002) Exchange of N-CoR corepressor and Tip60 coactivator complexes links gene expression by NF-κB and β-amyloid precursor protein. *Cell* **110,** 55–67
39. Checler, F., Sunyach, C., Pardossi-Piquard, R., Sévalle, J., Vincent, B., Kawarai, T., Girardot, N., St George-Hyslop, P., and da Costa, C. A. (2007) The γ/ε-secretase-derived APP intracellular domain fragments regulate p53. *Curr. Alzheimer Res.* **4,** 423–426
40. Leissring, M. A., Murphy, M. P., Mead, T. R., Akbari, Y., Sugarman, M. C., Jannatipour, M., Anliker, B., Müller, U., Saftig, P., De Strooper, B., Wolfe, M. S., Golde, T. E., and LaFerla, F. M. (2002) A physiologic signaling role for the γ-secretase-derived intracellular fragment of APP. *Proc. Natl. Acad. Sci. U.S.A.* **99,** 4697–4702
41. Müller, U. C., and Zheng, H. (2012) Physiological functions of APP family proteins. *Cold Spring Harb. Perspect. Med* **2,** a006288
42. Scheinfeld, M. H., Ghersi, E., Laky, K., Fowlkes, B. J., and D'Adamio, L. (2002) Processing of β-amyloid precursor-like protein-1 and -2 by γ-secretase regulates transcription. *J. Biol. Chem.* **277,** 44195–44201
43. Heber, S., Herms, J., Gajic, V., Hainfellner, J., Aguzzi, A., Rülicke, T., von Kretzschmar, H., von Koch, C., Sisodia, S., Tremml, P., Lipp, H. P., Wolfer, D. P., and Müller, U. (2000) Mice with combined gene knockouts reveal essential and partially redundant functions of amyloid precursor protein family members. *J. Neurosci.* **20,** 7951–7963
44. Herms, J., Anliker, B., Heber, S., Ring, S., Fuhrmann, M., Kretzschmar, H., Sisodia, S., and Müller, U. (2004) Cortical dysplasia resembling human type 2 lissencephaly in mice lacking all three APP family members. *EMBO J.* **23,** 4106–4115
45. von Koch, C. S., Zheng, H., Chen, H., Trumbauer, M., Thinakaran, G., van der Ploeg, L. H., Price, D. L., and Sisodia, S. S. (1997) Generation of APLP2 KO mice and early postnatal lethality in APLP2/APP double KO mice. *Neurobiol. Aging* **18,** 661–669
46. Scheinfeld, M. H., Matsuda, S., and D'Adamio, L. (2003) JNK-interacting protein-1 promotes transcription of Aβ protein precursor but not Aβ precursor-like proteins, mechanistically different than Fe65. *Proc. Natl. Acad. Sci. U.S.A.* **100,** 1729–1734
47. Wang, P., Yang, G., Mosier, D. R., Chang, P., Zaidi, T., Gong, Y. D., Zhao, N. M., Dominguez, B., Lee, K. F., Gan, W. B., and Zheng, H. (2005) Defective neuromuscular synapses in mice lacking amyloid precursor protein (APP) and APP-Like protein 2. *J. Neurosci.* **25,** 1219–1225
48. Del Prete, D., Lombino, F., Liu, X., and D'Adamio, L. (2014) APP is cleaved by Bace1 in pre-synaptic vesicles and establishes a pre-synaptic interactome, via its intracellular domain, with molecular complexes that regulate pre-synaptic vesicles functions. *PLoS One* **9,** e108576
49. Ito, T., Ando, H., Suzuki, T., Ogura, T., Hotta, K., Imamura, Y., Yamaguchi, Y., and Handa, H. (2010) Identification of a primary target of thalidomide teratogenicity. *Science* **327,** 1345–1350
50. Lombino, F., Biundo, F., Tamayev, R., Arancio, O., and D'Adamio, L. (2013) An intracellular threonine of amyloid-β precursor protein mediates synaptic plasticity deficits and memory loss. *PLoS One* **8,** e57120
51. Tamayev, R., and D'Adamio, L. (2012) Inhibition of γ-secretase worsens memory deficits in a genetically congruous mouse model of Danish dementia.. *Mol. Neurodegener.* **7,** 19
52. Riederer, B. M., Leuba, G., Vernay, A., and Riederer, I. M. (2011) The role of the ubiquitin proteasome system in Alzheimer's disease. *Exp. Biol. Med.* **236,** 268–276
53. Matrone, C., Luvisetto, S., La Rosa, L. R., Tamayev, R., Pignataro, A., Canu, N., Yang, L., Barbagallo, A. P., Biundo, F., Lombino, F., Zheng, H., Ammassari-Teule, M., and D'Adamio, L. (2012) Tyr682 in the Aβ-precursor protein intracellular domain regulates synaptic connectivity, cholinergic function, and cognitive performance. *Aging Cell* **11,** 1084–1093
54. Barbagallo, A. P., Weldon, R., Tamayev, R., Zhou, D., Giliberto, L., Foreman, O., and D'Adamio, L. (2010) Tyr(682) in the intracellular domain of APP regulates amyloidogenic APP processing *in vivo*. *PLoS One* **5,** e15503
55. Tamayev, R., Zhou, D., and D'Adamio, L. (2009) The interactome of the amyloid β precursor protein family members is shaped by phosphorylation of their intracellular domains. *Mol. Neurodegener.* **4,** 28
56. Zhou, D., Zambrano, N., Russo, T., and D'Adamio, L. (2009) Phosphor-

ylation of a tyrosine in the amyloid-β protein precursor intracellular domain inhibits Fe65 binding and signaling. *J. Alzheimers Dis.* **16,** 301–307
57. Ghersi, E., Vito, P., Lopez, P., Abdallah, M., and D'Adamio, L. (2004) The intracellular localization of amyloid β protein precursor (AβPP) intracellular domain associated protein-1 (AIDA-1) is regulated by AβPP and alternative splicing. *J. Alzheimers Dis.* **6,** 67–78
58. Ghersi, E., Noviello, C., and D'Adamio, L. (2004) Amyloid-β protein precursor (AβPP) intracellular domain-associated protein-1 proteins bind to AβPP and modulate its processing in an isoform-specific manner. *J. Biol. Chem.* **279,** 49105–49112
59. Zhou, D., Noviello, C., D'Ambrosio, C., Scaloni, A., and D'Adamio, L. (2004) Growth factor receptor-bound protein 2 interaction with the tyrosine-phosphorylated tail of amyloid β precursor protein is mediated by its Src homology 2 domain. *J. Biol. Chem.* **279,** 25374–25380
60. Scheinfeld, M. H., Ghersi, E., Davies, P., and D'Adamio, L. (2003) Amyloid β protein precursor is phosphorylated by JNK-1 independent of, yet facilitated by, JNK-interacting protein (JIP)-1. *J. Biol. Chem.* **278,** 42058–42063
61. Matsuda, S., Matsuda, Y., and D'Adamio, L. (2003) Amyloid β protein precursor (AβPP), but not AβPP-like protein 2, is bridged to the kinesin light chain by the scaffold protein JNK-interacting protein 1. *J. Biol. Chem.* **278,** 38601–38606
62. Noviello, C., Vito, P., Lopez, P., Abdallah, M., and D'Adamio, L. (2003) Autosomal recessive hypercholesterolemia protein interacts with and regulates the cell surface level of Alzheimer's amyloid β precursor protein. *J. Biol. Chem.* **278,** 31843–31847
63. Tarr, P. E., Roncarati, R., Pelicci, G., Pelicci, P. G., and D'Adamio, L. (2002) Tyrosine phosphorylation of the β-amyloid precursor protein cytoplasmic tail promotes interaction with Shc. *J. Biol. Chem.* **277,** 16798–16804
64. Roncarati, R., Sestan, N., Scheinfeld, M. H., Berechid, B. E., Lopez, P. A., Meucci, O., McGlade, J. C., Rakic, P., and D'Adamio, L. (2002) The γ-secretase-generated intracellular domain of β-amyloid precursor protein binds Numb and inhibits Notch signaling. *Proc. Natl. Acad. Sci. U.S.A.* **99,** 7102–7107
65. Scheinfeld, M. H., Roncarati, R., Vito, P., Lopez, P. A., Abdallah, M., and D'Adamio, L. (2002) Jun NH_2-terminal kinase (JNK) interacting protein 1 (JIP1) binds the cytoplasmic domain of the Alzheimer's β-amyloid precursor protein (APP). *J. Biol. Chem.* **277,** 3767–3775
66. Ciarlo, E., Massone, S., Penna, I., Nizzari, M., Gigoni, A., Dieci, G., Russo, C., Florio, T., Cancedda, R., and Pagano, A. (2013) An intronic ncRNA-dependent regulation of SORL1 expression affecting Aβ formation is upregulated in post-mortem Alzheimer's disease brain samples. *Dis. Model. Mech.* **6,** 424–433
67. Russo, C., Dolcini, V., Salis, S., Venezia, V., Zambrano, N., Russo, T., and Schettini, G. (2002) Signal transduction through tyrosine-phosphorylated C-terminal fragments of amyloid precursor protein via an enhanced interaction with Shc/Grb2 adaptor proteins in reactive astrocytes of Alzheimer's disease brain. *J. Biol. Chem.* **277,** 35282–35288
68. Duilio, A., Faraonio, R., Minopoli, G., Zambrano, N., and Russo, T. (1998) Fe65L2: a new member of the Fe65 protein family interacting with the intracellular domain of the Alzheimer's β-amyloid precursor protein. *Biochem. J.* **330,** 513–519
69. Fiore, F., Zambrano, N., Minopoli, G., Donini, V., Duilio, A., and Russo, T. (1995) The regions of the Fe65 protein homologous to the phosphotyrosine interaction/phosphotyrosine binding domain of Shc bind the intracellular domain of the Alzheimer's amyloid precursor protein. *J. Biol. Chem.* **270,** 30853–30856
70. Borg, J. P., Ooi, J., Levy, E., and Margolis, B. (1996) The phosphotyrosine interaction domains of X11 and FE65 bind to distinct sites on the YENPTY motif of amyloid precursor protein. *Mol. Cell. Biol.* **16,** 6229–6241
71. McLoughlin, D. M., and Miller, C. C. (1996) The intracellular cytoplasmic domain of the Alzheimer's disease amyloid precursor protein interacts with phosphotyrosine-binding domain proteins in the yeast two-hybrid system. *FEBS Lett.* **397,** 197–200
72. Lu, P. J., Wulf, G., Zhou, X. Z., Davies, P., and Lu, K. P. (1999) The prolyl isomerase Pin1 restores the function of Alzheimer-associated phosphorylated tau protein. *Nature* **399,** 784–788
73. Tamayev, R., Zhou, D., and D'Adamio, L. (2009) The interactome of the amyloid βη precursor protein family members is shaped by phosphorylation of their intracellular domains. *Mol. Neurodegener.* **4,** 28
74. Sang, Y., Yan, F., and Ren, X. (2015) The role and mechanism of CRL4 E3 ubiquitin ligase in cancer and its potential therapy implications. *Oncotarget* **6,** 42590–42602
75. Jackson, S., and Xiong, Y. (2009) CRL4s: the CUL4-RING E3 ubiquitin ligases. *Trends Biochem. Sci.* **34,** 562–570
76. Skaar, J. R., Pagan, J. K., and Pagano, M. (2014) SCF ubiquitin ligase-targeted therapies. *Nat. Rev. Drug Discov.* **13,** 889–903
77. Skaar, J. R., Pagan, J. K., and Pagano, M. (2013) Mechanisms and function of substrate recruitment by F-box proteins. *Nat. Rev. Mol. Cell Biol.* **14,** 369–381
78. Hotton, S. K., and Callis, J. (2008) Regulation of cullin RING ligases. *Annu. Rev Plant Biol* **59,** 467–489
79. Schwechheimer, C. (2004) The COP9 signalosome (CSN): an evolutionary conserved proteolysis regulator in eukaryotic development. *Biochim. Biophys. Acta* **1695,** 45–54
80. Dahlmann, B. (2016) Mammalian proteasome subtypes: their diversity in structure and function. *Arch. Biochem. Biophys.* **591,** 132–140
81. Coyne, E. S., and Wing, S. S. (2016) The business of deubiquitination-location, location, location. *F1000Res* **5,** F1000
82. Lee, D. Y., and Brown, E. J. (2012) Ubiquilins in the crosstalk among proteolytic pathways. *Biol. Chem.* **393,** 441–447
83. Russo, C., Venezia, V., Repetto, E., Nizzari, M., Violani, E., Carlo, P., and Schettini, G. (2005) The amyloid precursor protein and its network of interacting proteins: physiological and pathological implications. *Brain Res. Brain Res. Rev.* **48,** 257–264
84. Pastorino, L., Sun, A., Lu, P. J., Zhou, X. Z., Balastik, M., Finn, G., Wulf, G., Lim, J., Li, S. H., Li, X., Xia, W., Nicholson, L. K., and Lu, K. P. (2006) The prolyl isomerase Pin1 regulates amyloid precursor protein processing and amyloid-β production. *Nature* **440,** 528–534
85. Kumar, P., Ambasta, R. K., Veereshwarayya, V., Rosen, K. M., Kosik, K. S., Band, H., Mestril, R., Patterson, C., and Querfurth, H. W. (2007) CHIP and HSPs interact with β-APP in a proteasome-dependent manner and influence Aβ metabolism. *Hum. Mol. Genet.* **16,** 848–864
86. Rajadhyaksha, A. M., Ra, S., Kishinevsky, S., Lee, A. S., Romanienko, P., DuBoff, M., Yang, C., Zupan, B., Byrne, M., Daruwalla, Z. R., Mark, W., Kosofsky, B. E., Toth, M., and Higgins, J. J. (2012) Behavioral characterization of cereblon forebrain-specific conditional null mice: a model for human non-syndromic intellectual disability. *Behav. Brain Res.* **226,** 428–434
87. Hartmann, M. D., Boichenko, I., Coles, M., Zanini, F., Lupas, A. N., and Hernandez Alvarez, B. (2014) Thalidomide mimics uridine binding to an aromatic cage in cereblon. *J. Struct. Biol.* **188,** 225–232
88. Chamberlain, P. P., Lopez-Girona, A., Miller, K., Carmel, G., Pagarigan, B., Chie-Leon, B., Rychak, E., Corral, L. G., Ren, Y. J., Wang, M., Riley, M., Delker, S. L., Ito, T., Ando, H., Mori, T., *et al.* (2014) Structure of the human Cereblon-DDB1-lenalidomide complex reveals basis for responsiveness to thalidomide analogs. *Nat. Struct. Mol. Biol.* **21,** 803–809
89. Fischer, E. S., Böhm, K., Lydeard, J. R., Yang, H., Stadler, M. B., Cavadini, S., Nagel, J., Serluca, F., Acker, V., Lingaraju, G. M., Tichkule, R. B., Schebesta, M., Forrester, W. C., Schirle, M., Hassiepen, U., *et al.* (2014) Structure of the DDB1-CRBN E3 ubiquitin ligase in complex with thalidomide. *Nature* **512,** 49–53
90. Dawson, G. R., Seabrook, G. R., Zheng, H., Smith, D. W., Graham, S., O'Dowd, G., Bowery, B. J., Boyce, S., Trumbauer, M. E., Chen, H. Y., Van der Ploeg, L. H., and Sirinathsinghji, D. J. (1999) Age-related cognitive deficits, impaired long-term potentiation and reduction in synaptic marker density in mice lacking the β-amyloid precursor protein. *Neuroscience* **90,** 1–13
91. Norstrom, E. M., Zhang, C., Tanzi, R., and Sisodia, S. S. (2010) Identification of NEEP21 as a ss-amyloid precursor protein-interacting protein *in vivo* that modulates amyloidogenic processing *in vitro*. *J. Neurosci.* **30,** 15677–15685
92. Kohli, B. M., Pflieger, D., Mueller, L. N., Carbonetti, G., Aebersold, R.,

Nitsch, R. M., and Konietzko, U. (2012) Interactome of the amyloid precursor protein APP in brain reveals a protein network involved in synaptic vesicle turnover and a close association with Synaptotagmin-1. *J. Proteome Res.* **11,** 4075–4090
93. Sabbagh, J. J., and Dickey, C. A. (2016) The metamorphic nature of the tau protein: dynamic flexibility comes at a cost. *Front. Neurosci.* **10,** 3
94. Holtzman, D. M., Herz, J., and Bu, G. (2012) Apolipoprotein E and apolipoprotein E receptors: normal biology and roles in Alzheimer disease. *Cold Spring Harb. Perspect. Med.* **2,** a006312
95. Petrucelli, L., Dickson, D., Kehoe, K., Taylor, J., Snyder, H., Grover, A., De Lucia, M., McGowan, E., Lewis, J., Prihar, G., Kim, J., Dillmann, W. H., Browne, S. E., Hall, A., Voellmy, R., *et al.* (2004) CHIP and Hsp70 regulate τ ubiquitination, degradation and aggregation. *Hum. Mol. Genet.* **13,** 703–714
96. Shimura, H., Schwartz, D., Gygi, S. P., and Kosik, K. S. (2004) CHIP-Hsc70 complex ubiquitinates phosphorylated τ and enhances cell survival. *J. Biol. Chem.* **279,** 4869–4876
97. Islam, K., and Levy, E. (1997) Carboxyl-terminal fragments of β-amyloid precursor protein bind to microtubules and the associated protein τ. *Am. J. Pathol.* **151,** 265–271
98. Harris, F. M., Brecht, W. J., Xu, Q., Tesseur, I., Kekonius, L., Wyss-Coray, T., Fish, J. D., Masliah, E., Hopkins, P. C., Scearce-Levie, K., Weisgraber, K. H., Mucke, L., Mahley, R. W., and Huang, Y. (2003) Carboxyl-terminal-truncated apolipoprotein E4 causes Alzheimer's disease-like neurodegeneration and behavioral deficits in transgenic mice. *Proc. Natl. Acad. Sci. U.S.A.* **100,** 10966–10971
99. Brecht, W. J., Harris, F. M., Chang, S., Tesseur, I., Yu, G. Q., Xu, Q., Dee Fish, J., Wyss-Coray, T., Buttini, M., Mucke, L., Mahley, R. W., and Huang, Y. (2004) Neuron-specific apolipoprotein e4 proteolysis is associated with increased tau phosphorylation in brains of transgenic mice. *J. Neurosci.* **24,** 2527–2534
100. Wenner, C., Lorkowski, S., Engel, T., and Cullen, P. (2001) Apolipoprotein E in macrophages and hepatocytes is degraded via the proteasomal pathway. *Biochem. Biophys. Res. Commun.* **282,** 608–614
101. Morel, E., Chamoun, Z., Lasiecka, Z. M., Chan, R. B., Williamson, R. L., Vetanovetz, C., Dall'Armi, C., Simoes, S., Point Du Jour, K. S., McCabe, B. D., Small, S. A., and Di Paolo, G. (2013) Phosphatidylinositol-3-phosphate regulates sorting and processing of amyloid precursor protein through the endosomal system. *Nat. Commun.* **4,** 2250
102. Wang, Z., Wang, B., Yang, L., Guo, Q., Aithmitti, N., Songyang, Z., and Zheng, H. (2009) Presynaptic and postsynaptic interaction of the amyloid precursor protein promotes peripheral and central synaptogenesis. *J. Neurosci.* **29,** 10788–10801
103. Yang, G., Gong, Y. D., Gong, K., Jiang, W. L., Kwon, E., Wang, P., Zheng, H., Zhang, X. F., Gan, W. B., and Zhao, N. M. (2005) Reduced synaptic vesicle density and active zone size in mice lacking amyloid precursor protein (APP) and APP-like protein 2. *Neurosci. Lett.* **384,** 66–71
104. Li, M., Pehar, M., Liu, Y., Bhattacharyya, A., Zhang, S. C., O'Riordan, K. J., Burger, C., D'Adamio, L., and Puglielli, L. (2015) The amyloid precursor protein (APP) intracellular domain regulates translation of p44, a short isoform of p53, through an IRES-dependent mechanism. *Neurobiol. Aging* **36,** 2725–2736
105. Keller, J. N., Hanni, K. B., and Markesbery, W. R. (2000) Impaired proteasome function in Alzheimer's disease. *J. Neurochem.* **75,** 436–439
106. Tamayev, R., Matsuda, S., Arancio, O., and D'Adamio, L. (2012) β- but not γ-secretase proteolysis of APP causes synaptic and memory deficits in a mouse model of dementia. *EMBO Mol. Med.* **4,** 171–179
107. Liu, W., Meng, M., Zhang, B., Du, L., Pan, Y., Yang, P., Gu, Z., Zhou, Q., and Cao, Z. (2015) Dehydroeffusol effectively inhibits human gastric cancer cell-mediated vasculogenic mimicry with low toxicity. *Toxicol. Appl. Pharmacol.* **287,** 98–110
108. Cao, X., and Südhof, T. C. (2004) Dissection of amyloid-β precursor protein-dependent transcriptional transactivation. *J. Biol. Chem.* **279,** 24601–24611
109. Froyen, G., Corbett, M., Vandewalle, J., Jarvela, I., Lawrence, O., Meldrum, C., Bauters, M., Govaerts, K., Vandeleur, L., Van Esch, H., Chelly, J., Sanlaville, D., van Bokhoven, H., Ropers, H. H., Laumonnier, F., *et al.* (2008) Submicroscopic duplications of the hydroxysteroid dehydrogenase HSD17B10 and the E3 ubiquitin ligase HUWE1 are associated with mental retardation. *Am. J. Hum. Genet.* **82,** 432–443
110. Dijkhuizen, T., van Essen, T., van der Vlies, P., Verheij, J. B., Sikkema-Raddatz, B., van der Veen, A. Y., Gerssen-Schoorl, K. B., Buys, C. H., and Kok, K. (2006) FISH and array-CGH analysis of a complex chromosome 3 aberration suggests that loss of CNTN4 and CRBN contributes to mental retardation in 3pter deletions. *Am. J. Med. Genet. A.* **140,** 2482–2487
111. Higgins, J. J., Pucilowska, J., Lombardi, R. Q., and Rooney, J. P. (2004) A mutation in a novel ATP-dependent Lon protease gene in a kindred with mild mental retardation. *Neurology* **63,** 1927–1931
112. Londin, E. R., Adijanto, J., Philp, N., Novelli, A., Vitale, E., Perria, C., Serra, G., Alesi, V., Surrey, S., and Fortina, P. (2014) Donor splice-site mutation in CUL4B is likely cause of X-linked intellectual disability. *Am. J. Med. Genet. A* **164A,** 2294–2299
113. Badura-Stronka, M., Jamsheer, A., Materna-Kiryluk, A., Sowińska, A., Kiryluk, K., Budny, B., and Latos-Bieleńska, A. (2010) A novel nonsense mutation in CUL4B gene in three brothers with X-linked mental retardation syndrome. *Clin. Genet.* **77,** 141–144
114. Zou, Y., Liu, Q., Chen, B., Zhang, X., Guo, C., Zhou, H., Li, J., Gao, G., Guo, Y., Yan, C., Wei, J., Shao, C., and Gong, Y. (2007) Mutation in CUL4B, which encodes a member of cullin-RING ubiquitin ligase complex, causes X-linked mental retardation. *Am. J. Hum. Genet.* **80,** 561–566
115. Tarpey, P. S., Raymond, F. L., O'Meara, S., Edkins, S., Teague, J., Butler, A., Dicks, E., Stevens, C., Tofts, C., Avis, T., Barthorpe, S., Buck, G., Cole, J., Gray, K., Halliday, K., *et al.* (2007) Mutations in CUL4B, which encodes a ubiquitin E3 ligase subunit, cause an X-linked mental retardation syndrome associated with aggressive outbursts, seizures, relative macrocephaly, central obesity, hypogonadism, pes cavus, and tremor. *Am. J. Hum. Genet.* **80,** 345–352
116. Homan, C. C., Kumar, R., Nguyen, L. S., Haan, E., Raymond, F. L., Abidi, F., Raynaud, M., Schwartz, C. E., Wood, S. A., Gecz, J., and Jolly, L. A. (2014) Mutations in USP9X are associated with X-linked intellectual disability and disrupt neuronal cell migration and growth. *Am. J. Hum. Genet.* **94,** 470–478
117. Clark, L. N., Afridi, S., Mejia-Santana, H., Harris, J., Louis, E. D., Cote, L. J., Andrews, H., Singleton, A., Wavrant De-Vrieze, F., Hardy, J., Mayeux, R., Fahn, S., Waters, C., Ford, B., Frucht, S., Ottman, R., and Marder, K. (2004) Analysis of an early-onset Parkinson's disease cohort for DJ-1 mutations. *Mov. Disord.* **19,** 796–800
118. Clark, L. N., Afridi, S., Karlins, E., Wang, Y., Mejia-Santana, H., Harris, J., Louis, E. D., Cote, L. J., Andrews, H., Fahn, S., Waters, C., Ford, B., Frucht, S., Ottman, R., and Marder, K. (2006) Case-control study of the parkin gene in early-onset Parkinson disease. *Arch. Neurol.* **63,** 548–552
119. Hedrich, K., Djarmati, A., Schäfer, N., Hering, R., Wellenbrock, C., Weiss, P. H., Hilker, R., Vieregge, P., Ozelius, L. J., Heutink, P., Bonifati, V., Schwinger, E., Lang, A. E., Noth, J., Bressman, S. B., *et al.* (2004) DJ-1 (PARK7) mutations are less frequent than Parkin (PARK2) mutations in early-onset Parkinson disease. *Neurology* **62,** 389–394
120. Bonifati, V., Rizzu, P., van Baren, M. J., Schaap, O., Breedveld, G. J., Krieger, E., Dekker, M. C., Squitieri, F., Ibanez, P., Joosse, M., van Dongen, J. W., Vanacore, N., van Swieten, J. C., Brice, A., Meco, G., *et al.* (2003) Mutations in the DJ-1 gene associated with autosomal recessive early-onset parkinsonism. *Science* **299,** 256–259
121. Shi, Y., Wang, J., Li, J. D., Ren, H., Guan, W., He, M., Yan, W., Zhou, Y., Hu, Z., Zhang, J., Xiao, J., Su, Z., Dai, M., Wang, J., Jiang, H., *et al.* (2013) Identification of CHIP as a novel causative gene for autosomal recessive cerebellar ataxia. *PloS one* **8,** e81884
122. Heimdal, K., Sanchez-Guixé, M., Aukrust, I., Bollerslev, J., Bruland, O., Jablonski, G. E., Erichsen, A. K., Gude, E., Koht, J. A., Erdal, S., Fiskerstrand, T., Haukanes, B. I., Boman, H., Bjørkhaug, L., Tallaksen, C. M., *et al.* (2014) STUB1 mutations in autosomal recessive ataxias–evidence for mutation-specific clinical heterogeneity. *Orphanet J. Rare Dis.* **9,** 146
123. Depondt, C., Donatello, S., Simonis, N., Rai, M., van Heurck, R., Abramowicz, M., D'Hooghe, M., and Pandolfo, M. (2014) Autosomal recessive cerebellar ataxia of adult onset due to STUB1 mutations. *Neurology* **82,** 1749–1750

124. Cordoba, M., Rodriguez-Quiroga, S., Gatto, E. M., Alurralde, A., and Kauffman, M. A. (2014) Ataxia plus myoclonus in a 23-year-old patient due to STUB1 mutations. *Neurology* **83,** 287–288
125. Klein, C. J., Wu, Y., Vogel, P., Goebel, H. H., Bönnemann, C., Zukosky, K., Botuyan, M. V., Duan, X., Middha, S., Atkinson, E. J., Mer, G., and Dyck, P. J. (2014) Ubiquitin ligase defect by DCAF8 mutation causes HMSN2 with giant axons. *Neurology* **82,** 873–878
126. Frosk, P., Weiler, T., Nylen, E., Sudha, T., Greenberg, C. R., Morgan, K., Fujiwara, T. M., and Wrogemann, K. (2002) Limb-girdle muscular dystrophy type 2H associated with mutation in TRIM32, a putative E3-ubiquitin-ligase gene. *Am. J. Hum. Genet.* **70,** 663–672
127. Schoser, B. G., Frosk, P., Engel, A. G., Klutzny, U., Lochmüller, H., and Wrogemann, K. (2005) Commonality of TRIM32 mutation in causing sarcotubular myopathy and LGMD2H. *Ann. Neurol.* **57,** 591–595
128. Saccone, V., Palmieri, M., Passamano, L., Piluso, G., Meroni, G., Politano, L., and Nigro, V. (2008) Mutations that impair interaction properties of TRIM32 associated with limb-girdle muscular dystrophy 2H. *Hum. Mutat.* **29,** 240–247
129. Sell, G. L., and Margolis, S. S. (2015) From UBE3A to Angelman syndrome: a substrate perspective. *Front. Neurosci.* **9,** 322
130. Finsterer, J., and Burgunder, J. M. (2014) Recent progress in the genetics of motor neuron disease. *Eur. J. Med. Genet.* **57,** 103–112
131. Dlamini, N., Josifova, D. J., Paine, S. M., Wraige, E., Pitt, M., Murphy, A. J., King, A., Buk, S., Smith, F., Abbs, S., Sewry, C., Jacques, T. S., and Jungbluth, H. (2013) Clinical and neuropathological features of X-linked spinal muscular atrophy (SMAX2) associated with a novel mutation in the UBA1 gene. *Neuromuscul. Disord.* **23,** 391–398
132. Iqbal, Z., Willemsen, M. H., Papon, M. A., Musante, L., Benevento, M., Hu, H., Venselaar, H., Wissink-Lindhout, W. M., Vulto-van Silfhout, A. T., Vissers, L. E., de Brouwer, A. P., Marouillat, S., Wienker, T. F., Ropers, H. H., Kahrizi, K., *et al.* (2015) Homozygous SLC6A17 mutations cause autosomal-recessive intellectual disability with progressive tremor, speech impairment, and behavioral problems. *Am. J. Hum. Genet.* **96,** 386–396
133. Bourassa, C. V., Meijer, I. A., Merner, N. D., Grewal, K. K., Stefanelli, M. G., Hodgkinson, K., Ives, E. J., Pryse-Phillips, W., Jog, M., Boycott, K., Grimes, D. A., Goobie, S., Leckey, R., Dion, P. A., and Rouleau, G. A. (2012) VAMP1 mutation causes dominant hereditary spastic ataxia in Newfoundland families. *Am. J. Hum. Genet.* **91,** 548–552
134. Herrmann, D. N., Horvath, R., Sowden, J. E., Gonzalez, M., Gonzales, M., Sanchez-Mejias, A., Guan, Z., Whittaker, R. G., Almodovar, J. L., Lane, M., Bansagi, B., Pyle, A., Boczonadi, V., Lochmüller, H., Griffin, H., *et al.* (2014) Synaptotagmin 2 mutations cause an autosomal-dominant form of Lambert-Eaton myasthenic syndrome and nonprogressive motor neuropathy. *Am. J. Hum. Genet.* **95,** 332–339
135. Shen, X. M., Selcen, D., Brengman, J., and Engel, A. G. (2014) Mutant SNAP25B causes myasthenia, cortical hyperexcitability, ataxia, and intellectual disability. *Neurology* **83,** 2247–2255
136. Garcia, C. C., Blair, H. J., Seager, M., Coulthard, A., Tennant, S., Buddles, M., Curtis, A., and Goodship, J. A. (2004) Identification of a mutation in synapsin I, a synaptic vesicle protein, in a family with epilepsy. *J. Med. Genet.* **41,** 183–186
137. Saunders, A. M., Strittmatter, W. J., Schmechel, D., George-Hyslop, P. H., Pericak-Vance, M. A., Joo, S. H., Rosi, B. L., Gusella, J. F., Crapper-MacLachlan, D. R., and Alberts, M. J. (1993) Association of apolipoprotein E allele ϵ4 with late-onset familial and sporadic Alzheimer's disease. *Neurology* **43,** 1467–1472
138. Baizabal-Carvallo, J. F., and Jankovic, J. (2016) Parkinsonism, movement disorders and genetics in frontotemporal dementia. *Nat. Rev. Neurol.* **12,** 175–185
139. Iqbal, K., Liu, F., and Gong, C. X. (2016) Tau and neurodegenerative disease: the story so far. *Nat. Rev. Neurol.* **12,** 15–27
140. Thomas, S. N., Cripps, D., and Yang, A. J. (2009) Proteomic analysis of protein phosphorylation and ubiquitination in Alzheimer's disease. *Methods Mol. Biol.* **566,** 109–121
141. Cripps, D., Thomas, S. N., Jeng, Y., Yang, F., Davies, P., and Yang, A. J. (2006) Alzheimer disease-specific conformation of hyperphosphorylated paired helical filament-Tau is polyubiquitinated through Lys-48, Lys-11, and Lys-6 ubiquitin conjugation. *J. Biol. Chem.* **281,** 10825–10838
142. Morris, M., Knudsen, G. M., Maeda, S., Trinidad, J. C., Ioanoviciu, A., Burlingame, A. L., and Mucke, L. (2015) Tau post-translational modifications in wild-type and human amyloid precursor protein transgenic mice. *Nat. Neurosci.* **18,** 1183–1189
143. Lim, K. L. (2007) Ubiquitin-proteasome system dysfunction in Parkinson's disease: current evidence and controversies. *Expert Rev. Proteomics* **4,** 769–781